BASAL FOREBRAIN GABAERGIC PROJECTIONS TO THE AMYGDALA AND THE BNST IN WISTAR RATS

TUĞÇE TUNA

BOĞAZİÇİ UNIVERSITY

2021

BASAL FOREBRAIN GABAERGIC PROJECTIONS TO THE AMYGDALA AND THE BNST IN WISTAR RATS

Thesis submitted to the
Institute for Graduate Studies for Social Sciences
in partial fulfillment of the requirements for the degree of

Master of Arts
in
Psychological Sciences

by
Tuğçe Tuna

Boğaziçi University
2021

DECLARATION OF ORIGINALITY

I, Tuğçe Tuna, certify that

- I am the sole author of this thesis and that I have fully acknowledged and documented in my thesis all sources of ideas and words, including digital resources, which have been produced or published by another person or institution;
- this thesis contains no material that has been submitted or accepted for a degree or diploma in any other educational institution;
- this is a true copy of the thesis approved by my advisor and thesis committee at Boğaziçi University, including final revisions required by them.

Signature……

Date……

ABSTRACT

Basal Forebrain GABAergic Projections to the Amygdala and the BNST in Wistar Rats

Medial septal GABAergic neurons of the basal forebrain selectively innervate GABAergic interneurons in the hippocampus and form a disinhibitory circuit. This long-range GABAergic projection contributes to hippocampal theta oscillations (4-12 Hz), which correlate with hippocampal forms of learning and memory including spatial navigation. I postulate that basal forebrain-driven disinhibition creates a general neuromodulation for limbic structures. Basal forebrain GABAergic projections to the amygdala and the bed nucleus of the stria terminalis (BNST), structures respectively encoding phasic and sustained fear (anxiety), may be a key regulator of their local network activities. Testing this calls for an anatomical description of the basal forebrain GABAergic projections to the amygdala and the BNST. This thesis provides a detailed description of the projections as well as several projecting subpopulations by utilizing retrograde tract-tracing and fluorescent immunohistochemistry in Wistar rats. Tracing showed that the substantia innominata/sublenticular extended amygdala (SI/EA), the ventral pallidum (VP), and the nucleus of the horizontal limb of the diagonal band/magnocellular preoptic nucleus (hDB/MCPO) project to the amygdala and the BNST. Immunohistochemistry revealed calbindin (CB)- and parvalbumin (PV)-immunopositive putative GABAergic subpopulations among the projecting neurons.

ÖZET

Wistar Sıçanlarında Amigdala ve BNST'ye Bazal Önbeyin GABAerjik Projeksiyonları

Bazal önbeynin medial septal çekirdeğinden GABAerjik nöronlar hipokampüste seçici olarak GABAerjik aranöronları innerve ederler ve bir disinhibitör devre oluştururlar. Bu uzun menzilli GABAerjik projeksiyon, mekânsal navigasyon da dahil olmak üzere hipokampal öğrenme ve bellek tipleriyle korele olan hipokampal teta osilasyonlarına (4-12 Hz) katkı sağlar. Bu çalışmada, bazal önbeyin kaynaklı disinhibisyonun limbik bölgeler için genel bir nöromodülasyon oluşturduğu ileri sürülmektedir. Sırasıyla kısa ve uzun vadeli korku (anksiyete) edinimi sağlayan amigdala ve stria terminalis yatak çekirdeği (BNST)'ye giden bazal önbeyin GABAerjik projeksiyonları bu bölgelerin lokal ağ faaliyetleri için önemli bir regülatör olabilir. Bunu test etmek, bazal önbeyinden amigdala ve BNST'ye giden GABAerjik projeksiyonların anatomik betimlemesini gerektirmektedir. Bu tez Wistar sıçanlarında retrograd nöronal boyama ve floresan immünohistokimya kullanarak bu projeksiyonların ve birkaç projeksiyon altgrubunun detaylı bir betimlemesini sağlamaktadır. Nöronal boyama, substantia innominata/genişletilmiş amigdala (SI/EA), ventral pallidum (VP) ve Broca'nın diagonal çekirdeği/magnocelüler preoptik çekirdeğin (hDB/MCPO) amigdala ve BNST'ye projeksiyon gönderdiğini göstermiştir. İmmünohistokimya projeksiyon gönderen nöronlar arasında calbindin (CB)- ve parvalbumin (PV)-immünpozitif altgruplar ortaya çıkarmıştır.

ACKNOWLEDGEMENTS

I would like to extend my biggest thanks to my PI Assist. Prof. Güneş Ünal for introducing me to the field of systems neuroscience. We met through the PSY 48B course he gave in his first semester as a professor in Bogazici University. That course completely changed my mind for what I want for my career and helped me to find the path that I am truly passionate about. I still remember vividly what I learned in that course. I joined the Psychobiology Lab thanks to him and I will always be proud of being a part of that wonderful lab founded by Emeritus Prof. Reşit Canbeyli. We made the transition to the Behavioral Neuroscience Lab together and created an amazing lab environment which I will miss wherever I go. Thank you again for all your support, mentorship, and availability. I will always feel special for being one of the first master's students of yours.

Thanks to Emeritus Prof. Reşit Canbeyli, Assist. Prof. Elif Aysimi Duman, Assist. Prof. Mehmet Kocatürk, Assist. Prof. Efe Soyman, and Assist. Prof. İnci Ayhan for being in my thesis committee. I appreciate your time and all the valuable feedback you provided to my study. Special thanks to Emeritus Prof. Reşit Canbeyli and Assist. Prof. İnci Ayhan for their help during my PhD application process.

Thanks to the Psychology Department, especially to my advisors Prof. Ayşecan Boduroğlu and Assist. Prof. Esra Mungan. Also, thanks to Prof. Adil Sarıbay, Assist. Profs. Güneş Ünal, Gaye Soley, and Nur Soylu Yalçınkaya, and to Nur Yeniçeri for amazing master's courses they gave. I learned a lot from you.

I love neuroscience because lab members make it so much fun. I cannot express enough how thankful I am to all the Behavioral Neuroscience Lab members. Merve Akan, thank you for being my closest friend from the beginning and for all your

support and help. I will miss our coffee breaks. Cemal Akmeşe, thank you for all your solutions to make things work better in the lab and thank you for making me laugh all the time. Here, also thanks to Emirhan Albayrak for his fun presence in the lab and for the coverslips he provided for me. Dilan Gökalp, thank you for being the best RA ever. You always made things run smoothly in the lab. Also, thanks for your help in cresyl violet staining. Oğuz Nas, Covid19 set physical distances between us but thank you for your friendship. Aybüke Akkaya, also thank you for your friendship and for all your help in my surgeries. Thank you Sahar Halim for our fun chats. I hope the best for you in Boğaziçi and in İstanbul. Ege Kingir and Cem Sevinç, I cannot think you separately, so I will thank you at the same time. Thank you for your curiosity in my work and for all your amazing questions. I certainly learned from you and I hope I could teach you, as well. Arda Ateş and Hüma Erbörü, thank you for being the coolest undergrads in the lab. All the other newest members including Deren Aykan, Selçuk Polat, and Salih Çayır, thank you for your help in my work and thank you for your questions. You made me realize that I love teaching as well as research. I will miss having lunch and talking science with all of you. You have been the best!

I could not survive the first year of master's without the support of my amazing cohort. Special thanks to our assistants Derya Karademir and Beliz Korkut for answering patiently all my technical questions and for their friendship. I will miss having lunch with you. Thank you Özlem Şahin for being the most conscious and thoughtful person I have ever known. Thank you Rüya Su Şencan, Burcu Avcı, Büşranur Güllü, Ege Kamber, Mertcan Güngör, Arif Yasin Kavdır, and Gizem Dal for being great friends and making master's much easier. I know you will all be doing incredible work in the future and I feel proud for having colleagues like you.

Thank you to my beautiful friends Tuğçe Koç, Perim Uyar, and Selin Uysal for all their support during this process. You made Boğaziçi so much more meaningful for me. Thank you my “angels” for believing in me, being on my side, and making me laugh all the time. Special thanks to your support during lockdown, you have been providing the best break. Our holidays together will always be the most fun activities of my life.

Thank you to my friends Sümeyye Yücel and Sümeyye Burhan and to my twin sister Ayça Tuna for being my support system in academia. I look up to your studiousness and professional stance as future academics. You are making me proud with your progress and I cannot wait to see your future work. Our trips abroad made me study more to have incredible holidays as a reward. They will always be the best experiences of my life and I want to have more of them in the future.

Finally, I want to thank to my sisters Ayça Tuna and Beril Tuna and to my mother and father Sevim and Barış Tuna for always being supportive of my education and career goals.

TABLE OF CONTENTS

LIST OF FIGURES

ABBREVIATIONS

3V	3rd ventricle
AA	Anterior amygdaloid area
ac	Anterior commissure
aca	Anterior commissure, anterior part
acp	Anterior commissure, posterior part
ACo	Anterior cortical amygdaloid nucleus
AHA	Anterior hypothalamic area, anterior part
AhiAL	Amygdalohippocampal area, anterolateral part
AM	Anteromedial thalamic nucleus
BLA	Basolateral amygdaloid nucleus, anterior part
BLP	Basolateral amygdaloid nucleus, posterior part
BLV	Basolateral amygdaloid nucleus, ventral part
BMA	Basomedial amygdaloid nucleus, anterior part
BMP	Basomedial amygdaloid nucleus, posterior part
BNST	Bed nucleus of the stria terminalis
CB	Calbindin
CBP	Calcium-binding protein
cc	Corpus callosum

CeA	Central amygdaloid nuclei
CeC	Central amygdaloid nucleus, capsular part
CeL	Central amygdaloid nucleus, lateral part
CeM	Central amygdaloid nucleus, medial part
CeMAV	Central amygdaloid nucleus, medial anteroventral part
ChAT	Choline acetyltransferase
CPu	Caudate putamen
CR	Calretinin
CRF	Corticotropin-releasing factor
CS	Conditioned stimulus
CxA	Cortex-amygdala transition zone
DEn	Dorsal endopiriform nucleus
dH_2O	Distilled H_20
EA	Extended amygdala
EAC	Sublenticular extended amygdala, central part
EAM	Sublenticular extended amygdala, medial part
ec	External capsule
EtOH	Ethanol
FB	Fast blue
GABA	Gamma-aminobutyric acid

GAD	Glutamic acid decarboxylase
GP	Globus pallidus
hDB/MCPO	Nucleus of the horizontal limb of the diagonal band/Magnocellular preoptic nucleus
HRP	Horseradish peroxidase
I	Intercalated nuclei of the amygdala
ic	Internal capsule
i.p.	Intraperitoneal
IPAC	Interstitial nucleus of the posterior limb of the anterior commissure
IPACL	Interstitial nucleus of the posterior limb of the anterior commissure, lateral part
IPACM	Interstitial nucleus of the posterior limb of the anterior commissure, medial part
LA	Lateral amygdaloid nucleus
LaDL	Lateral amygdaloid nucleus, dorsolateral part
LaVL	Lateral amygdaloid nucleus, ventrolateral part
LaVM	Lateral amygdaloid nucleus, ventromedial part
LPO	Lateral preoptic area
LV	Lateral ventricle
MeA	Medial amygdaloid nuclei

MePD	Medial amygdaloid nucleus, posterodorsal part
MePV	Medial amygdaloid nucleus, posteroventral part
MPA	Medial preoptic area
MPO	Medial preoptic nucleus
MPOL	Medial preoptic nucleus, lateral part
MPOM	Medial preoptic nucleus, medial part
MS/vDB	Medial septum/Nucleus of the vertical limb of the diagonal band
NGS	Normal goat serum
NHS	Normal horse serum
NY	Nuclear yellow
PAG	Phosphate-activated glutaminase
PB	Phosphate buffer
PBS	Phosphate-buffered saline
PBS-TX	Phosphate-buffered saline-Triton X-100
PFA	Paraformaldehyde
PHAL	Phaseolus vulgaris leucoagglutinin
PLH	Peduncular part of lateral hypothalamus
PT	Paratenial thalamic nucleus
PV	Parvalbumin
PVA	Paraventricular thalamic nucleus, anterior part

SATB1	Special AT-rich sequence-binding protein-1
s.c.	Subcutaneous
SI	Substantia innominata
SIB	Substantia innominata, basal part
SO	Supraoptic nucleus
SOM	Somatostatin
st	Stria terminalis
STLD	Bed nucleus of the stria terminalis, lateral division, dorsal part
STLI	Bed nucleus of the stria terminalis, lateral division, intermediate part
STLJ	Bed nucleus of the stria terminalis, lateral division, juxtacapsular part
STLP	Bed nucleus of the stria terminalis, lateral division, posterior part
STLV	Bed nucleus of the stria terminalis, lateral division, ventral part
STMA	Bed nucleus of the stria terminalis, medial division, anterior part
STMPI	Bed nucleus of the stria terminalis, medial division, posterointermediate part
STMPL	Bed nucleus of the stria terminalis, medial division, posterolateral part
STMPM	Bed nucleus of the stria terminalis, medial division, posteromedial part
STMV	Bed nucleus of the stria terminalis, medial division, ventral part
US	Unconditioned stimulus

VGAT	Vesicular GABA transporter
VGluT2	Vesicular glutamate transporter 2
VGluT3	Vesicular glutamate transporter 3
VLPO	Ventrolateral preoptic nucleus
VP	Ventral pallidum
WGA-HRP	Wheat-germ-agglutinin-conjugated horseradish peroxidase

CHAPTER 1

INTRODUCTION

Fear constitutes one of our six basic emotions (Ekman, 1992). It is crucial for survival, rapidly emerging in the face of an immediate threat and ending with a species-specific response such as freezing. When the threat is no longer present, the fear ceases. A sustained form of fear, known as anxiety, on the other hand, may emerge with the presence of a less certain threat (i.e. when the source of the threat is not known or is known to be far away), and may be experienced for a longer period of time. Produced by overlapping neuronal mechanisms, fear and anxiety are respectively called phasic fear and sustained fear in neuroscience research (Davis, Walker, Miles, & Grillon, 2010; Walker, Miles, & Davis, 2009).

Extreme and dysfunctional forms of phasic and sustained fear are encountered in different forms of psychopathology. According to the Diagnostic and Statistical Manual of Mental Disorders-5 (DSM-5), depressive disorders involve fear of the past events, while anxiety disorders involve fear of potential future events. Trauma- and stressor-related disorders, on the other hand, involve abnormal levels of acute stress and fear (American Psychiatric Association, 2013).

Basic research revealing neuronal circuits underlying phasic and sustained forms of fear is necessary to better target these disorders and increase treatment efficiency. Contemporary neuroscience has techniques such as chemogenetics (Armbruster, Li, Pausch, Herlitze, & Roth, 2007) and optogenetics (Deisseroth, 2011; Yizhar, Fenno, Zhang, Hegemann, & Diesseroth, 2011) to make cell-type specific manipulations in the brain. In the future, drugs that selectively target specific

neuronal types will replace classical pharmacological agents that often lead to several side effects (Kennedy, 2006; Riediger et al., 2017; Wang et al., 2018).

This thesis presents an anatomical investigation of the subcircuits and neuronal groups underlying phasic and sustained fear. It is a descriptive study within the novel neuroscientific framework as it provides the first step to understand the role of the described subcircuits and neuronal groups using aforementioned neuroscientific techniques. Studies will follow to selectively activate or silence the described subcircuits and neuronal groups using chemogenetics and the effects of this activation or silencing on animals' fear and anxiety related learning and memory processes will be observed.

1.1 Amygdala

In the mammalian brain, fear and anxiety are mediated by the amygdala and the bed nucleus of the stria terminalis (BNST), respectively (Davis et al., 2010; Walker et al., 2009). Both structures are part of the limbic system, which refers to a collection of cortical and subcortical structures that regulate emotions, motivation, olfaction, and different types of memory (MacLean, 1949). This section will focus on the amygdala.

The amygdala is a limbic system structure receiving cortical and thalamic input with emotional valence, including those regarding fear. It has more than 10 major nuclei (Figure 1) collectively known as the amygdaloid complex (Sah, Faber, Lopez De Armentia, & Power, 2003). Weiskrantz (1956) showed that ablations of the amygdaloid complex in monkeys prevented demonstration of fear. Ablations also increased the time to acquire conditioned avoidance and conditioned depression and

decreased the time required for the extinction of preoperatively acquired conditioned avoidance responses.

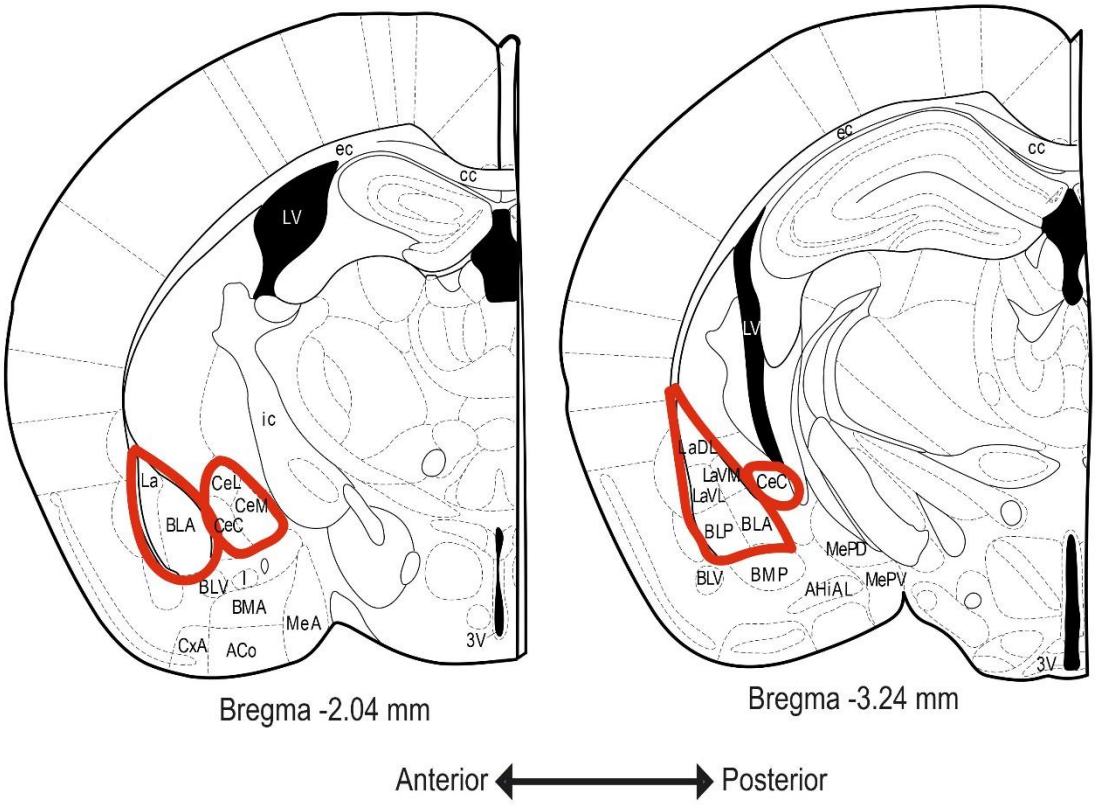

Fig. 1 Amygdala nuclei
Note: Almond shaped red enclosed nuclei constitute the basolateral complex. Circular shaped nuclei next to the basolateral amygdala constitute the central amygdala. Coronal maps are adapted from Paxinos and Franklin (2001). Refer to abbreviations

Inputs to the amygdala enter the complex through the basolateral group. Basolateral group includes lateral (LA), basolateral (BLA), and basomedial (BMA) nuclei (Pitkänen, Savander, & LeDoux, 1997; Sah et al., 2003). These nuclei are heterogeneous in terms of their cellular makeup. While pyramidal-like excitatory neurons are the principal cell type, different inhibitory interneuron types exist including those containing parvalbumin (PV), calbindin (CB), calretinin (CR), somatostatin (SOM), or a combination of these (McDonald, 2020; McDonald &

Mascagni, 2002; McDonald, Mascagni, & Zaric, 2012; McDonald, Muller, & Mascagni, 2011). Basolateral nuclei send their output to central amygdaloid nuclei (CeA). Central amygdaloid nuclei are the main output center of the basolateral group and include lateral (CeL), capsular (CeC), and medial (CeM) parts (Pitkänen et al., 1997; Sah et al., 2003). Many GABAergic neurons reside in the central amygdaloid nuclei including those containing several neuropeptides such as enkephalin, neurotensin, and corticotropin releasing hormone (Day, Curran, Watson Jr., & Akil, 1999; Sun & Cassell, 1993; Swanson & Petrovich, 1998). From the central amygdaloid nucleus, medial part (CeM), information is relayed to several hypothalamic and brainstem nuclei, which in turn, leads to rapid hormonal changes and behavioral output for phasic fear response (Pitkänen et al., 1997; Sah et al., 2003). For instance, input to the lateral hypothalamus is key for the regulation of changes in blood pressure while input to the periaqueductal gray is key for freezing response (LeDoux, Iwata, Cicchetti, & Reis, 1988). Another major output center of the amygdaloid complex is the BNST (Dong, Petrovich, & Swanson, 2001) which will be described in more detail in the next section.

1.2 The bed nucleus of the stria terminalis

The bed nucleus of the stria terminalis (BNST) is located rostrally and dorsomedially to the amygdala. The BNST, similar to the amygdaloid complex, is composed of several subnuclei including anterior, posterior, medial, intermediate, lateral, dorsal, ventral, and juxtacapsular parts and divisions (Ju & Swanson, 1989; Moga, Saper, & Gray, 1989) (Figure 2). It is implicated in stress regulation (Casada & Dafny, 1991; Henke, 1984) and autonomic functions (Gray & Magnuson, 1987; Sofroniew, 1983)

in addition to anxiety (Fendt, Endres, & Apfelbach, 2003; Silveira, Sandner, & Graeff, 1993). Pioneering studies from our laboratory showed that bilateral lesions of the BNST in Wistar rats reduce freezing behavior during uncontrollable and inescapable stress (Schulz & Canbeyli, 1999) and increase depressive-like behavior in forced swim test without affecting navigational learning in water maze (Pezuk, Aydin, Aksoy, & Canbeyli, 2008; Pezük, Göz, Aksoy, & Canbeyli, 2006; Schulz & Canbeyli, 2000). These results suggested that the BNST integrity is required for adaptive coping response in the face of uncontrollable and inescapable stress as well as long duration stress and are in line with the BNST's involvement in sustained forms of fear.

From the amygdala, especially the central nuclei, neuronal information regarding anxiety, or sustained fear, is selectively relayed to the BNST. The two structures are connected to each other following the axonal fibers known as the stria terminalis (Johnston, 1923). The connection from the centromedial amygdala to the BNST through the sublenticular substantia innominata is called the "extended amygdala'' (Alheid, 2003; Alheid & Heimer, 1988; Alheid & Heimer, 1996). Sustained threat activates the central amygdaloid nucleus, lateral part (CeL) which then releases corticotropin-releasing factor (CRF) to the lateral division of the BNST. CRF, a peptide involved in stress response, is selectively released for sustained fear, but not phasic fear. Released CRF binds to its receptors in the lateral division of the BNST. The BNST, then, relays information to the same hypothalamic and brainstem nuclei as the amygdala to produce sustained fear response (for reviews see Davis et al., 2010; Walker et al., 2009).

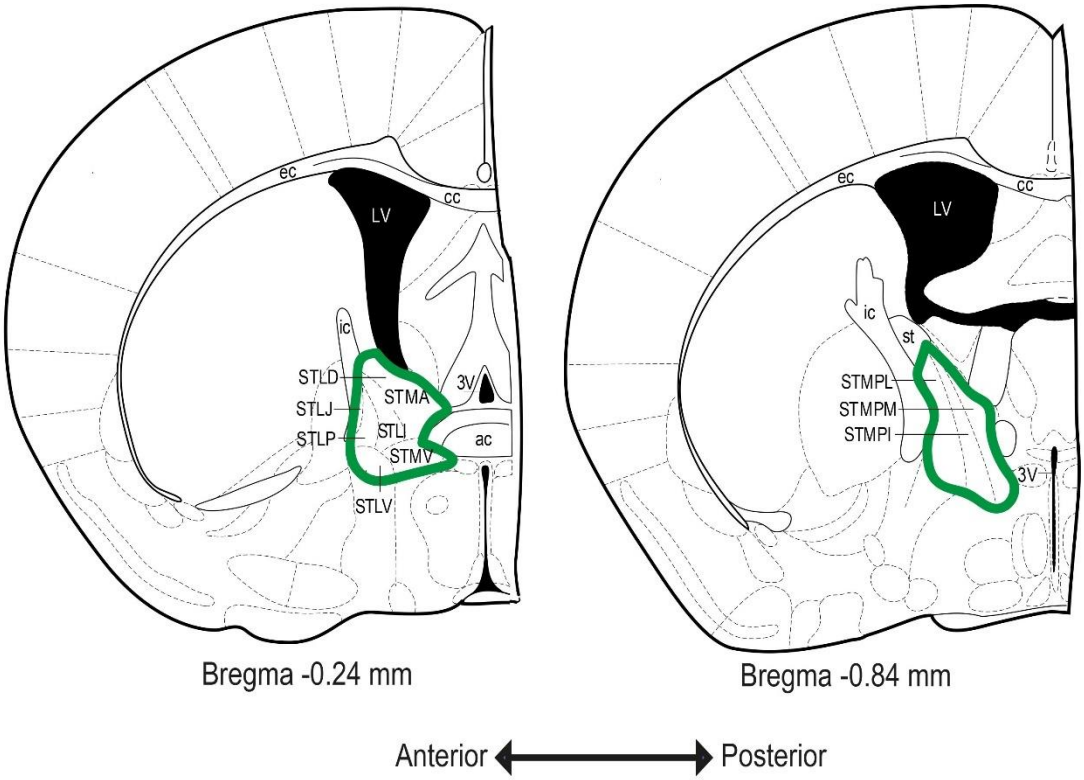

Fig. 2 BNST nuclei
Note: Green enclosed nuclei constitute the BNST. Coronal maps are adapted from Paxinos and Franklin (2001). Refer to abbreviations

1.3 Differential roles of the amygdala and the BNST in phasic vs. sustained fear

The amygdala gets activated in response to a threat to provide an acute fear response. However, it also gets activated in response to a threat that leads to a sustained fear response. It sends the necessary input to the BNST which then sends input to several hypothalamic and brainstem nuclei (Walker et al., 2009). Walker et al. (2009) hypothesized that the BNST also sends input back to the amygdala to shut down its activity. Through this feedback mechanism, the amygdala's recruitment during sustained fear is ended while the BNST takes over to produce sustained fear response.

Many studies have combined amygdala and BNST lesions with different phasic and sustained fear paradigms and showed differential involvement of the amygdala and the BNST in phasic vs. sustained fear responses (for a review see Davis et al., 2010). Fear-potentiated startle is a common phasic fear paradigm whereas light-enhanced startle is used as a sustained fear paradigm. Fear-potentiated startle paradigm exposes animals to a brief and certain threat. It is a conditioning paradigm in which brief presentations of a conditioned stimulus (CS), usually a light or tone, is paired with a noxious unconditioned stimulus (US), usually a foot shock. After the conditioning, animals are presented with noise bursts in the presence vs. absence of the CS and the acoustic startle responses are measured (Brown, Kalish, & Farber, 1951; Davis et al., 2010). Light-enhanced startle, on the other hand, exposes animals to a longer lasting uncertain threat. Rats are nocturnal animals which prefer dark over light and they feel safer in dark environments compared to brightly lit environments (File & Hyde, 1978; Richter, 1922). Light-enhanced startle paradigm takes advantage of this natural preference. In this paradigm, acoustic startle response amplitudes are measured in two phases of 20 minutes each. In the first phase, rats are kept at dark. In the second phase, they are either kept at dark again, or transferred to a brightly lit place. Startle responses in the first and second phase are compared and increased startle magnitudes are observed for rats going from dark to light (Davis et al., 2010; Walker & Davis, 1997). Hitchcock and Davis (1986, 1991) showed that bilateral electrolytic lesions of the central amygdala block fear-potentiated startle in rats while similar lesions to the lateral BNST do not. However, infusions of the AMPA receptor antagonist NBQX to the lateral BNST block light-enhanced startle while similar infusions to the central amygdala do not (Davis et al., 2010).

Although the CeM and the lateral BNST differ in their functions in phasic and sustained fear, it is not possible to suggest a complete differentiation or double dissociation (for a review see Gungor & Paré, 2016). CRF release to the lateral BNST from the CeL is considered key for sustained fear response (Walker et al., 2009). In addition, although the CeM and the lateral BNST are differentially involved in phasic vs. sustained fear as mentioned above, both have a common input center, the BLA. BLA provides input not only to the CeM (Sah et al., 2003) but also to the lateral BNST (Dong, Petrovich, & Swanson, 2001; Krettek & Price, 1978) and disruption of the BLA also disrupts phasic and sustained fear responses. Lesions of the BLA block both fear-potentiated and light-enhanced startle (Davis et al., 2010).

1.4 Basal forebrain

As detailed in the prior section, the amygdala and the BNST have differential, and complementary, functions in fear and anxiety paradigms (for reviews see Davis et al., 2010; Walker et al., 2009) which require a precise coordination at the network level. A key structure implicated in coordinating the versatile limbic system activity encompassing several structures is the basal forebrain. Basal forebrain refers to several subcortical nuclei (Figure 3) located at the ventral forebrain. The medial septum (MS), vertical and horizontal limbs of the diagonal band (vDB and hDB), the ventral pallidum (VP), the substantia innominata (SI), and the sublenticular extended amygdala (EA) are basal forebrain nuclei, which differ in their neuronal connections, cytoarchitectural properties, and histochemical profiles (Zaborsky, Pang, Somogyi, Nadasdy, & Kallo, 1999; Zaborszky, van den Pol, & Gyengesi, 2012).

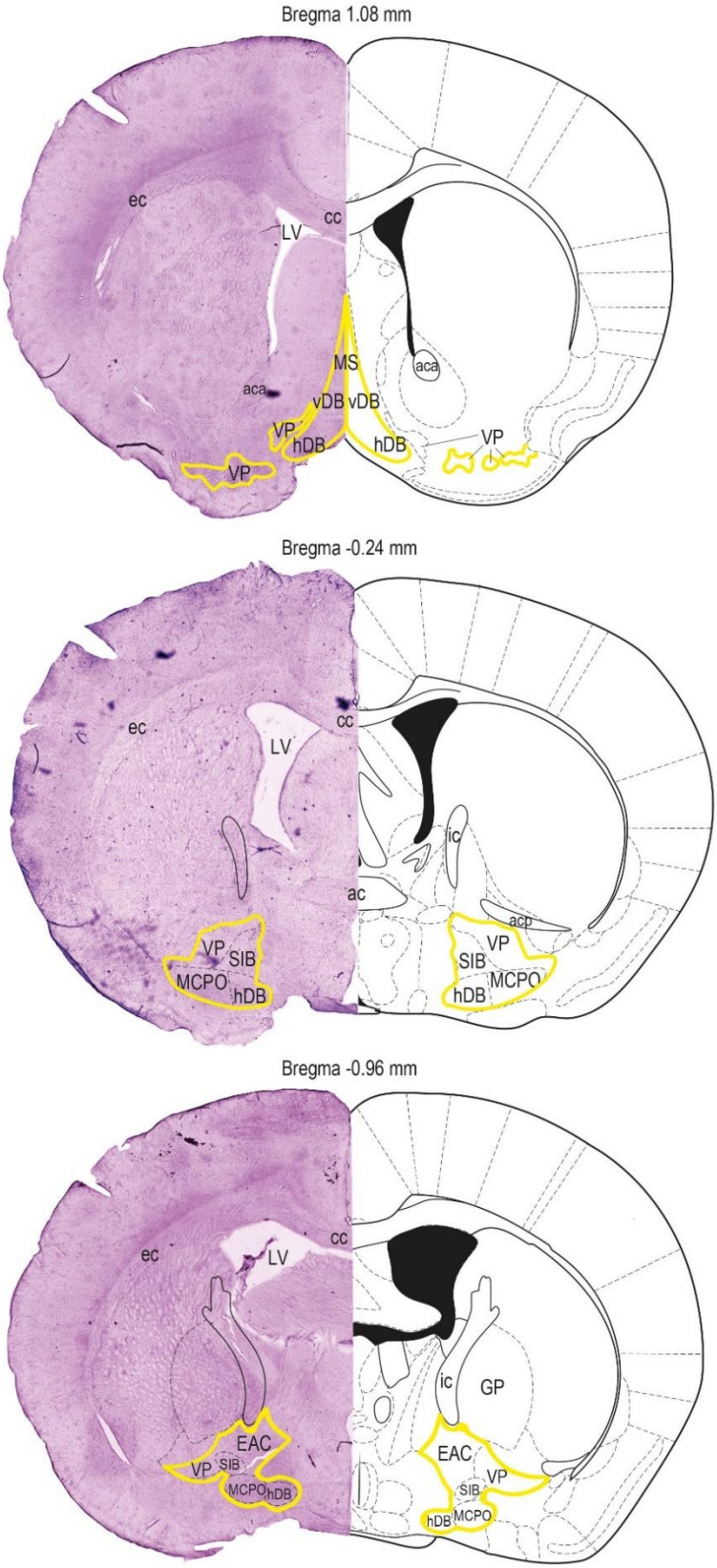

Fig. 3 Basal forebrain nuclei
Note: Yellow enclosed nuclei constitute the basal forebrain. Sections stained with cresyl violet on the left. Coronal maps on the right are adapted from Paxinos and Franklin (2001). Refer to abbreviations

Basal forebrain is the center of acetylcholine production. Acetylcholine is a neuromodulator distributed from the basal forebrain to the cortex and several subcortical structures via long-range axons (Mesulam, Mufson, Wainer, & Levey, 1983). In Alzheimer's disease, cortex-projecting cholinergic neurons are degenerated leading to memory problems (Mesulam, 2004). Overall, basal forebrain projections are known to be crucial for the coordination and modulation of cortical states, attention/vigilance, and several forms of learning and memory (Buzsaki et al., 1988; Cape, Manns, Alonso, Beaudet, & Jones, 2000; Durkin, 1989; Everitt & Robbins, 1997; Hassani, Lee, Henny, & Jones, 2009; Richardson & DeLong, 1988, 1991; Záborszky, Cullinan, & Braun, 1991).

Although basal forebrain projections were thought to be mostly cholinergic, several ablation studies demonstrated that the selective lesioning of cholinergic cells is not more detrimental compared to lesioning of other basal forebrain cell populations (Gerashchenko, Salin-Pascual, & Shiromani, 2001; Lee, Chrobak, Sik, Wiley, & Buzsáki, 1994). In addition to the cholinergic population, basal forebrain nuclei host glutamatergic (containing the usually excitatory neurotransmitter glutamate), GABAergic (containing the usually inhibitory neurotransmitter gamma-aminobutyric acid) and several peptidergic (containing neuropeptides) neurons (Brauer et al., 1991; Dinopoulos, Parnavelas, Uylings, & van Eden, 1988; Zaborsky et al., 1999). A stereological study by Gritti et al. (2006) indicated that the cholinergic cell population does not constitute the majority in the basal forebrain. Within the rat basal forebrain, the total number of cells was estimated to be ~355,000. Of these cells, only ~5% were found to be cholinergic with a number of ~22,000 (Gritti et al., 2006). Results of these lesioning and stereology research increased interest in the GABAergic cell population of the basal forebrain. So far,

basal forebrain GABAergic cell population and GABAergic projections have been studied extensively in relation to the hippocampus (Freund & Antal, 1988; Köhler, Chan-Palay, & Wu, 1984; Salib et al., 2019; Sun et al., 2014; Tóth, Freund, & Miles, 1997; Unal et al., 2018; Unal, Joshi, Viney, Kis, & Somogyi, 2015; Viney et al., 2013)**.** Next chapter will describe the role of basal forebrain projections in modulating limbic system activity by focusing on basal forebrain projections to the hippocampus. It will then explain the theory and specific hypotheses of the present study.

CHAPTER 2

LITERATURE REVIEW

2.1 Basal forebrain projections to the hippocampus

The hippocampus, another limbic system structure and the center of declarative (semantic and episodic) memory and spatial navigation (Eichenbaum, 2017; O'Keefe & Recce, 1993; Whishaw & Vanderwolf, 1973), receives both cholinergic and GABAergic projections from the medial septal nucleus of the basal forebrain (Baisden, Woodruff, & Hoover, 1984; Freund, 1989; Lewis & Shute, 1967; Wainer, Levey, Rye, Mesulam, & Mufson, 1985). These projections differ in target selectivity and function. While the cholinergic projection targets both pyramidal neurons and interneurons (Frotscher & Léránth, 1985), the GABAergic projection targets exclusively GABAergic interneurons and constitutes a disinhibitory circuit (Freund & Buzsáki, 1996; Freund & Antal, 1988). Many types of inhibitory interneuron in the hippocampus form inhibitory synapses with glutamatergic (often excitatory) pyramidal cells, which are the principal cells of the hippocampus. When the interneurons are inhibited by the basal forebrain GABAergic projection, they cannot inhibit their target cells. Therefore, this projection becomes indirectly excitatory for the pyramidal cells (Freund & Antal, 1988; Pascual, Pérez-Sust, & Soriano, 2004; Unal et al., 2018, 2015). In addition, GABAergic projection exerts its effect on target cells by directly sending inhibitory input while cholinergic neurons exert their effect slowly after binding to G-protein-coupled receptors. Therefore, while cholinergic projections are important for synaptic plasticity (Hasselmo, 2006), GABAergic projections are hypothesized to be crucial for the generation of network

oscillations (Hangya, Borhegyi, Szilágyi, Freund, & Varga, 2009) by assembling neuronal groups into coordinated activity (Somogyi, Katona, Klausberger, Lasztóczi, & Viney, 2014).

The long-range basal forebrain GABAergic projection from the medial septum indeed contributes to the generation of hippocampal theta oscillations (4-12 Hz) (Gerashchenko et al., 2001; Hangya et al., 2009; Lee et al., 1994; Yoder & Pang, 2005), which correlate with spatial navigation and other forms of hippocampal learning and memory (Klausberger & Somogyi, 2008). When septal projection is cut/lesioned, hippocampal theta loses oscillatory power and animals have difficulty with spatial navigation and other hippocampal learning and memory tasks (McNaughton, Ruan, & Woodnorth, 2006; Mizumori, Perez, Alvarado, Barnes, & McNaughton, 1990; Winson, 1978). In a related study by Mizumori, Perez, Alvarado, Barnes, and McNaughton (1990), rats were trained in an eight-arm radial maze spatial working memory task and tested after a 30 minutes delay. A local anesthetic, tetracaine, was injected to the medial septum to block its projections. Tetracaine injections before the training or the test phase increased error rates. In addition, intracranial EEG recordings showed that the inactivation of medial septal inputs temporarily reduced hippocampal theta. In parallel, McNaughton, Ruan, and Woodnorth (2006) demonstrated that similar tetracaine injections to the medial septum prevented learning in the Morris water maze which is a spatial learning and memory task (Morris, 1981). Interestingly however, restoring theta-like rhythmicity by means of oscillatory electrical stimulation also restored learning (McNaughton, Ruan, & Woodnorth, 2006).

Although findings above suggest a role for medial septal projections in hippocampal theta oscillations and hippocampal learning and memory, they do not

make a distinction between cholinergic and GABAergic projections. Tetracaine injection blocks both cholinergic and GABAergic components of the medial septal projections to the hippocampus. However, there is also direct evidence implicating the GABAergic component in the generation of hippocampal theta oscillations. Gerashchenko et al. (2001) contrasted the effects of lesioning cholinergic only and cholinergic as well as GABAergic medial septal neurons on hippocampal theta oscillations. Medial septal injections of 192 IgG–saporin lesioned only cholinergic neurons which led to a reduced theta activity. On the other hand, injections of hypocretin-saporin lesioned both cholinergic and GABAergic parvalbumin neurons which led to a complete loss of hippocampal theta activity. Lee et al. (1994) showed similar sparing of parvalbumin-immunopositive neurons with medial septal injections of 192 IgG-saporin. They similarly concluded that hippocampal neuronal activity stays in theta range, although reduced in power, following 192 IgG-saporin injections. These studies suggest that the medial septal GABAergic projection is necessary for hippocampal theta oscillations.

More recent studies using transgenic animals and optogenetics yielded similar results. Vandecasteele et al. (2014) selectively activated cholinergic medial septal neurons in ChAT-Cre mice and examined hippocampal local field potentials. This activation blocked sharp wave ripples, decreased the power of slow wave oscillations, and increased the power of theta oscillations. The results were similar for both anesthetized and behaving mice. Gangadharan et al. (2016) selectively activated parvalbumin-containing septohippocampal fibers in the dorsal fornix in PV-Cre mice from which medial septal projections reach the hippocampus. This activation increased object exploration behavior which is correlated with theta

oscillations. On the other hand, selective inhibition of the same fibers decreased object exploration behavior.

2.2 Basal forebrain projections to the amygdala and the BNST

Several tract-tracing studies showed that there are projections to the amygdala and the BNST from the basal forebrain, particularly from the ventral pallidum (VP) and the substantia innominata (SI) for the former and from the SI for the latter (Grove, 1988a, 1988b; Haber, Groenewegen, Grove, & Nauta, 1985; Ottersen, 1980). Ottersen (1980) injected the retrograde tracer horseradish peroxidase (HRP) to the amygdala in rats. Results showed that the VP projects to the LA and the BLA whereas the SI projects to the amygdaloid complex in its entirety, avoiding the LA. Haber et al. (1985) described efferent connections of the VP in the rat in an autoradiographic study. In line with the findings by Ottersen (1980), they showed VP fibers in the amygdala, especially in the BLA. They confirmed this finding by wheat-germ-agglutinin-conjugated HRP (WGA-HRP) injection to the BLA, which labeled neurons in the VP. In a subsequent study, the same group performed tracing to reveal the efferent connections of the VP in rats. Injections of the anterograde tracer phaseolus vulgaris leucoagglutinin (PHAL) to the VP labeled fibers mostly in the basolateral nuclei (Groenewegen, Berendse, & Haber, 1993). Similarly, Grove (1988a) described efferent connections of the SI in rats combining PHAL with WGA-HRP. PHAL injections to the dorsal SI labeled fibers in the LA, the BLA, and the CeA in addition to the lateral BNST. PHAL injections to the ventral SI, on the other hand, labeled fibers in the MeA and the medial BNST.

In a different study, Grove (1988b) examined afferent connections of the SI in rat combining PHAL and WGA-HRP tracing. Results showed that SI projections to the amygdala and the BNST are reciprocated. WGA-HRP injections to the dorsal SI revealed afferents from the amygdala and the BNST. Specifically, there were projections from the lateral BNST, CeM, and the BLA. Similar injections to the ventral SI revealed afferents from the medial BNST and medial and ventral amygdala. PHAL injections to the CeL revealed fibers in the dorsal SI and the lateral BNST while similar injections to the CeM revealed fibers in the ventral SI. PHAL injections to the lateral BNST revealed fibers in the dorsal SI, CeM, and basolateral nuclei while injections to the medial BNST revealed fibers in the ventral SI and ventromedial amygdaloid nuclei.

A key study by Carlsen, Záborszky, and Heimer (1985) combined retrograde tracing with immunohistochemistry to describe basal forebrain cholinergic projection to the BLA. Injections of the retrograde tracers Fast Blue (FB) and Nuclear Yellow (NY) to the BLA in rats led to labeling in the VP and the SI. Subsequent immunohistochemical staining for choline acetyltransferase (ChAT) and glutamic acid decarboxylase (GAD) revealed both cholinergic and GABAergic projection neurons in the same basal forebrain nuclei. Seventy-five percent of these amigdalopetal projections were cholinergic while twenty-five percent were noncholinergic. Mascagni and McDonald (2009) similarly performed retrograde tracing and immunohistochemistry to describe basal forebrain GABAergic projection to the basolateral complex. Injections of the retrograde tracer Fluorogold to the basolateral complex labeled neurons in the VP and the SI. Subsequent immunohistochemical staining for PV and GAD revealed that approximately 10-15% of the retrogradely labeled neurons are GABAergic. These studies suggest that the

basal forebrain GABAergic projection to the amygdala is not as dense compared to the basal forebrain cholinergic projection.

McDonald et al. (2011) combined anterograde tracing, immunohistochemistry, and electron microscopic observations to describe the postsynaptic targets of the basal forebrain GABAergic projection to the amygdala. PHAL injections into the VP and the SI revealed fibers in the basolateral nucleus including GABAergic ones. These GABAergic fibers selectively innervated GABAergic interneurons of the amygdala, especially PV-immunopositive interneurons. Basal forebrain cholinergic projection to the amygdala, on the other hand, selectively contacted glutamatergic principal neurons while only 10% of this input innervated GABAergic interneurons (Muller, Mascagni, & McDonald, 2011). This result suggests that the GABAergic projection creates a similar disinhibitory mechanism in the amygdala as in the hippocampus (Freund & Antal, 1988; Tóth et al., 1997). Although not being as numerous compared to basal forebrain cholinergic projection neurons, GABAergic ones gain the ability to influence the network processing in the amygdala by directly inhibiting GABAergic interneurons and disinhibiting principal neurons.

2.3 Present study

Mascagni and McDonald (2009) revealed that approximately 10% of the basal forebrain GABAergic neurons projecting to the amygdala are PV-immunopositive. More recently, Agostinelli, Geerling, and Scammell (2019) described basal forebrain GABAergic projections to subcortical structures including the amygdala and the BNST with anterograde tracing in vesicular GABA transporter (VGAT)-Cre mice.

However, this study did not make a distinction for different GABAergic subgroups. Do et al. (2016) performed anterograde tracing in PV-Cre and SOM-Cre transgenic mice and showed that a small proportion of SOM-immunopositive basal forebrain neurons project to the basolateral and basomedial amygdaloid nuclei. However, to date, a detailed description of other basal forebrain GABAergic subpopulations projecting to the amygdala has not been undertaken. Much less is known about the basal forebrain GABAergic projection to the BNST. Based on the pattern observed in the hippocampus and the amygdala, it is likely that a basal forebrain GABAergic projection predominantly, if not exclusively, targets GABAergic interneurons in the BNST. Do et al. (2016) also showed that a small proportion of PV- and SOM-immunopositive basal forebrain neurons project to the BNST. Presumably, many other BNST-projecting basal forebrain GABAergic subpopulations are yet to be described.

Present study aims to fill in these gaps in the literature for testing the following theory in subsequent studies combining chemogenetics and rodent behavioral testing. I postulate that basal forebrain GABAergic projections have a neuromodulatory role for limbic system structures which contribute to their local network oscillations and related learning and memory functions. As in the hippocampus, basal forebrain GABAergic projections selectively, although not exclusively, target GABAergic interneurons in the amygdala and the BNST, forming a disinhibitory circuit, which underlie their local network oscillations and phasic and sustained fear learning and memory processes.

This thesis is a neuroanatomical description study that will serve the end of testing the aforementioned postulation. I hypothesize that basal forebrain GABAergic projections selectively target GABAergic interneurons in the amygdala

and disinhibit the principal cells. As in the case of the hippocampus, the disinhibition of the principal cells contributes to phasic fear memory and behavior. Similarly, basal forebrain GABAergic projections selectively target GABAergic interneurons in the BNST and the emerging disinhibition contributes to sustained fear memory and behavior. To this end, this study describes basal forebrain GABAergic projections to the amygdala and the BNST in adult male Wistar rats. Stereotaxic surgeries were performed for retrograde tract-tracing from the amygdala and the BNST. Labeled neurons in basal forebrain nuclei were described. Subsequent immunohistochemistry for several neuronal markers revealed putative GABAergic subpopulations within the projecting neuronal groups. Stereological counting of the projecting neurons as well as those immunopositive for GABAergic markers was undertaken. The anatomical description made in this study provides the first step to test the aforementioned hypotheses at the functional level.

CHAPTER 3

MATERIAL AND METHODS

3.1 Subjects

Adult male Wistar rats (260-397 g; n = 16) were used in stereotaxic surgeries for retrograde tract-tracing. Animals were housed in cages of four with *ad libitum* access to food and water in a temperature- and humidity-controlled vivarium (21 ± 1 °C; 40 – 60 % humidity; 12:12 day/night cycle with lights on at 7:00 AM). All procedures were approved by Boğaziçi University Institutional Ethics Committee for the Local Use of Animals in Experiments (BÜHADYEK) (see Appendix A).

3.2 Stereotaxic surgeries

For recording surgeries, a stereotaxic surgery log sheet was used (see Appendix B). Animals were anesthetized with intraperitoneal (i.p.) injection of a mixture of ketamine (80 mg/kg) and xylazine (13.3 mg/kg). Following the complete loss of reflexes, heads were shaved and animals were head-fixed to a stereotaxic frame (Kopf Instruments) with the help of ear bars. An eye cream was applied to prevent drying. Throughout the surgeries, muscle reflexes were checked regularly, and if necessary, additional anesthetic was injected. A heating pad and an infrared heat lamp were utilized to keep the body temperature at approximately 36 °C. After the use of an additional local anesthetic (Vemcaine, 10% lidocaine) and antiseptic (Batticon), the skull was exposed through a vertical incision. Exposed surgical site was cleaned with saline and the Bregma point was located with a surgical

microscope. Injection coordinates determined beforehand using a rat brain atlas were calculated in reference to the Bregma point (LA: AP = −2.80, ML = ±5.30, DV = −7.30; BLA: AP = −2.80, ML = ±4.60, DV = −8.20; CeA: AP = −2.40, ML = ±4.20, DV = −8.00; MeA: AP = −2.16, ML = ±3.40, DV = −8.60; BNST: AP = −0.8, ML = ±1.50, DV = −6.40) (Paxinos & Watson, 2007). Two unilateral craniotomies were performed in line with the anterior-posterior (AP) and medial-lateral (ML) coordinates of target nuclei. In each brain, both the amygdala and the BNST were targeted. The injection syringe was lowered slowly to the desired depth along the dorsal-ventral (DV) axis as calculated in reference to the dura mater. Retrograde tracer was injected slowly and the syringe was retrieved ten minutes afterwards in order to prevent the dorsal diffusion of the tracer. Injection hemispheres were counterbalanced such that injections were in the right hemisphere in half of the animals and in the left hemisphere for the other half. After the injections were completed and the syringes were retrieved, the skull was cleaned and the incision was sutured. Local anesthetics (Anestol pomade, 5% lidocaine and Jetokain, 5 mg/kg, s.c.) and antiseptic (Batticon) were applied to the stitch. To prevent possible dehydration during the surgery, animals were injected with saline (2 ml, i.p.). They were then taken to the post-operative care during which they were regularly observed until waking up. In the following days, they were observed each day for scoring their general clinical symptoms, physical condition of the operation site, and behavioral symptoms of pain using a post-operative assessment checklist (see Appendix C). The amount of food and water consumption were recorded each day. Animals were injected an additional dose of Jetokain (5 mg/kg, s.c.) in cases of indications of pain.

3.3 Retrograde tract-tracing and Retrobeads

Tract-tracing is based on the axonal transport of tracers. Anterograde tracers refer to the tracers that are taken up by cell bodies at the site of injection and are carried towards terminal boutons following anterograde axonal transport. On the other hand, retrograde tracers are taken up by terminal boutons at the site of injection and are carried towards cell bodies following retrograde axonal transport. Retrograde tracers advance to cell bodies along the microtubules in axons through dynein's driving force (Oztas, 2003).

In the present study, retrograde tract-tracing was achieved with Retrobeads (Lumafluor Inc., USA). Retrobeads are fluorescent latex microspheres which appear as small beads within cell bodies once taken up (Apps & Ruigrok, 2007; Katz, Burkhalter, & Dreyer, 1984; Katz & Iarovici, 1990). Retrobeads have several characteristics that are appropriate for the purposes of this study. Most importantly, they have two color options, red and green. Using both colors, it was possible to target both the amygdala and the BNST in the same brain. Labeled neurons following the axonal transport could be observed in the same basal forebrain nuclei in different colors. In addition, Retrobeads show low diffusibility, high sensitivity, and high resistance to fading. That is, they do not diffuse extensively at the site of injection, they label a high number of cells, and labeling is resistant to fading over time. Furthermore, Retrobeads do not lead to anterograde labeling and are not toxic to the animals (Apps & Ruigrok, 2007; Katz et al., 1984; Schofield, 2008).

In each animal, colors of the tracer were counterbalanced between injection sites. In half of the animals, red beads were injected to the amygdala and green beads were injected to the BNST. In the other half, this pattern was reversed. Red (diluted

1:2 in saline; 200 nl) and green (undiluted; 200 nl) beads were pressure injected slowly using Hamilton microsyringes (1 μL) (Schofield, 2008) (Figure 4).

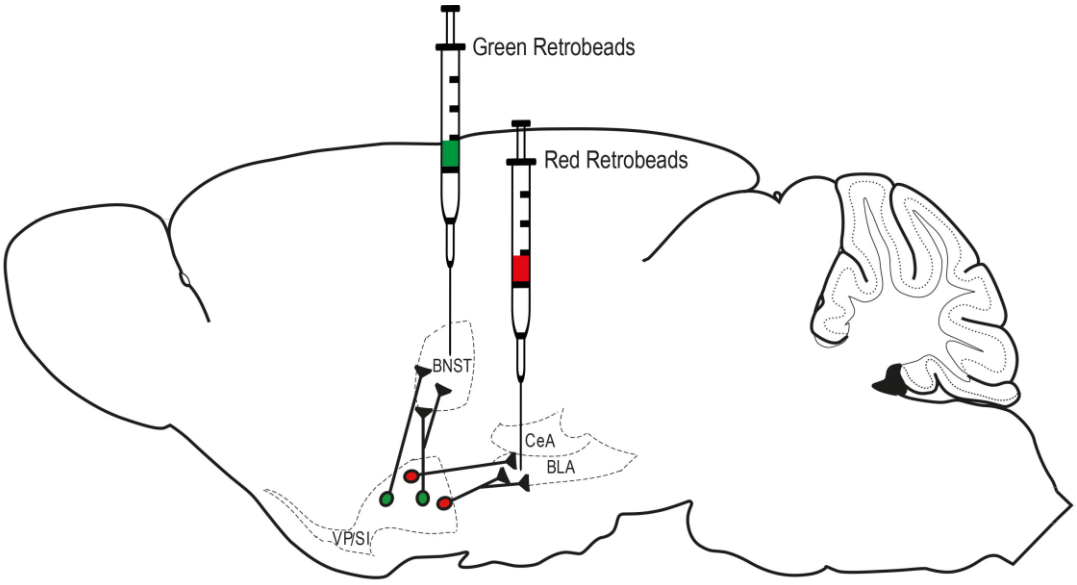

Fig. 4 Retrograde tract-tracing
Note: Red and green beads labeled cell bodies in VP/SI nuclei of the basal forebrain following red Retrobeads injection to the amygdala and green Retrobeads injection to the BNST. Refer to abbreviations

3.4 Histology and microscopic observations

Following the surgeries, animals were allowed to recover for 2-7 days. This time period was sufficient for the axonal transport of the tracers to be completed. At the end of this period, animals were transcardially perfused with 4% depolymerized paraformaldehyde (PFA) in saline. Brains were obtained and postfixed in 4% PFA for 1-2 overnights at 4 °C. They were then rinsed in 0.1 M phosphate-buffer (PB) three times, ten minutes each, on shaker. Coronal (frontal) sections of 60-80 μm thickness were cut using a Leica VT1000 S vibratome.

Initially, sections were observed for the injection sites using an Olympus BX43 epifluorescence microscope. Those brains with injection sites within the target

amygdala and/or BNST nuclei were further observed for labeled neurons in basal forebrain nuclei. To visualize red and green beads, sections were excited using green and blue filters, respectively. Neurons labeled with red and green beads in basal forebrain nuclei demonstrated projections from these nuclei to the amygdala and the BNST. Sections were then processed with immunohistochemical staining to characterize the molecular profiles of labeled projecting neurons of the basal forebrain.

3.5 Immunohistochemistry

Immunohistochemistry is a widely used method to localize and visualize biomarkers in the brain. It is based on specific binding of antibodies to their antigens. In this method, the marker of interest (e.g. parvalbumin) is introduced to a species (i.e. host) such as mouse, guinea pig, rabbit, and goat. The antibody (i.e. primary antibody) that the host's immune system produces as a response is collected (e.g. rabbit anti-parvalbumin). A secondary antibody is raised in a different host against immunoglobulins of the primary antibody's host and is conjugated with fluorophores (e.g. goat anti-rabbit 488). Secondary antibody specifically binds to the primary antibody. Incubating brain sections to a primary antibody raised against a marker of interest leads to the binding of the antibody to its antigen. Then, incubating sections to a secondary antibody leads to the binding of the secondary antibody to the primary one. By observing sections under a microscope using the appropriate fluorescent filter, neurons containing the marker of interest can be visualized (Coons, 1958; Hewitt, Baskin, Frevert, Stahl, & Rosa-Molinar, 2014; Saper, 2008).

In the present study, retrogradely labeled red and green neurons were tested for parvalbumin (PV) and calbindin (CB) immunoreactivities using a polyclonal rabbit anti-PV antibody (1:2000 dilution; code: ab11427; Abcam), a rabbit anti-PV antibody (1:5000 dilution; Swant), and a rabbit anti-CB antibody (1:1000 dilution; code: 230115; Swant). PV and CB are calcium-binding proteins (CBPs) that are usually expressed in GABAergic neurons and therefore, are used as GABAergic markers (Ivana Gritti, Manns, Mainville, & Jones, 2003; Unal et al., 2018, 2015; Viney et al., 2018; Zaborszky et al., 2012). Additionally, basal forebrain sections were immunostained for special AT-rich sequence-binding protein-1 (SATB1) and leu-enkephalin with a goat anti-SATB1 antibody (1:1000 dilution; Santa Cruz) and a polyclonal rabbit anti-Leu-enkephalin antibody (1:1000 dilution; code: ab22619; Abcam) (Table 1). SATB1 is a transcription factor that is expressed in a subgroup of PV-containing GABAergic interneurons in the hippocampus (Unal et al., 2018; Viney et al., 2013). Leu-enkephalin, on the other hand, is a regional marker for the VP. It does not label cell bodies but labels fibers and was used to differentiate the borders of the VP from neighboring nuclei (Smith & Berridge, 2005; Zahm, 1989). Specificity of the antibodies were checked with positive controls in prior immunohistochemical staining. Positive controls were processed with brain sections containing antigens of interest (Hewitt et al., 2014). These yielded specific binding of antibodies to their antigens. In addition, another set of brain sections were incubated to secondary antibodies in the absence of primary antibodies. No staining was observed in these sections. Overall, neither of the antibodies used in this study showed non-specificity.

Table 1. Primary Antibodies

Molecule	Host	Dilution	Source
PV	Rabbit	1:2000	Abcam, code: ab11427
PV	Rabbit	1:5000	Swant
CB	Rabbit	1:1000	Swant, code: 230115
SATB1	Goat	1:1000	Santa Cruz
Leu-enkephalin	Rabbit	1:1000	Abcam, code: ab22619

According to the standard single-labeling protocol, sections of 60-80 μm thickness were rinsed three times, for 10 minutes each, in phosphate-buffered saline containing 0.3% Triton X-100 (PBS-TX) to achieve tissue penetration. Then, blocking took place to prevent non-specific binding of antibodies. Sections were incubated in the blocking solution containing PBS-TX and 20% normal horse serum/normal goat serum (NHS/NGS) for an hour at room temperature. NHS or NGS were chosen depending on the species that the secondary antibody was raised in. Following blocking, sections were incubated in the primary antibody solution containing PBS-TX, 1% NHS/NGS, and primary antibodies diluted at specified ratios (see Table 1), for three nights at 4 °C. Following this step, they were rinsed in PBS-TX three times, for 10 minutes each. Then, they were incubated in the secondary antibody solution containing PBS-TX, 1% NHS/NGS, and secondary antibodies diluted at specified ratios for four hours at room temperature. At this step, slices were kept in the dark to prevent bleaching of secondary antibodies' fluorescence due to light exposure. All rinsing and incubation steps took place on a shaker. After a final rinse in PBS-TX three times, for 10 minutes each, sections were

mounted and coverslipped using the mounting medium methyl salicylate (Sigma-Aldrich).

3.6 Cresyl violet staining

To identify different basal forebrain nuclei and their borders, Nissl (cresyl violet) staining was utilized in addition to the rat brain atlas (Paxinos & Watson, 2007) (see Figure 3). Nissl staining is a nucleic acid staining technique that enables the visualization of cell bodies throughout the brain and is widely used to differentiate between brain regions and subcortical nuclei (Kádár, Wittmann, Liposits, & Fekete, 2009; Nissl, 1894; Pilati, Barker, Panteleimonitis, Donga, & Hamann, 2008).

Basal forebrain sections were taken from two brains that were not used for immunohistochemistry staining. These brains did not show much retrograde labeling. Sections were mounted on slides three days before the staining and heated for a minute right before the staining to prevent them from falling off. Cresyl violet solution was prepared beforehand by stirring 500 ml distilled H_2O (dH_2O), 0.5 g cresyl violet acetate, and 15 ml acetic acid for 24 h under fume hood. After that, the solution was filtered. According to the standard protocol, slides were passed through the following steps: 100% ethanol (EtOH) (two minutes), xylene I (two minutes), xylene II (two minutes), 100% EtOH (two minutes), 70% EtOH (two minutes), 20% EtOH (two minutes), dH_2O (one minute), cresyl violet solution (15 minutes), differentiation solution containing 70% EtOH and 10% acetic acid (two dips), differentiation solution containing 100% EtOH and 10% acetic acid (two dips), 100% EtOH (five minutes), xylene I (five minutes), and xylene II (five minutes). In all steps except for the differentiation solutions, racks holding the slides were gently

shaken in solutions. Slides were then coverslipped using Entellan New mounting medium (Merck).

3.7 Anatomical description

Basal forebrain nuclei were examined under the epifluorescence microscope. Retrogradely labeled red and green cell bodies in different basal forebrain nuclei were counted. Every second section in each brain was used for counting. As there was not heavy labeling in basal forebrain nuclei, counting was made manually by scanning the nuclei of interest under epifluorescence microscope with 20x magnification. Cell counts were then used to create graphs. Both total and normalized numbers were depicted in pie charts, separately for the amygdala and BNST injections. Total numbers were obtained by summing the number of cell bodies in each basal forebrain nucleus of each brain. Normalized numbers were obtained by dividing the total number observed in each nucleus of each brain by the number of sections observed for each nucleus. Numbers were then averaged across brains.

Similar counting was made following immunohistochemistry staining. Cell bodies expressing specific markers were counted in addition to retrogradely labeled red and green cell bodies. Those showing overlap (i.e. double-labeling) were noted. Using these numbers, percentages were calculated for single- and double-labeling for each marker tested. In addition, the number of single- and double-labeled neurons in each basal forebrain nucleus was demonstrated with bar graphs. Nuclei showing the highest number of double-labeling for specific markers were mapped on schemes of coronal basal forebrain sections. Coronal maps were created such that the location of

each cell body depicted on the scheme indicates its actual position in that nucleus in close approximation. That way, basal forebrain neurons projecting to the amygdala and the BNST and putative GABAergic subgroups within them were visualized.

Photomicrographs were obtained using Olympus cellSens Imaging Software (Ver. 2.2) and were edited using Adobe Photoshop (22.3.1). All figures, including the coronal maps, were created using Adobe Illustrator (25.0). Pie charts and bar graphs were created using Microsoft Excel.

CHAPTER 4

RESULTS

4.1 Injection sites

Classification of injection sites in amygdala and BNST nuclei was made based on the rat brain atlas of Paxinos and Watson (2007). Decision to include the brains for further processing (microscopic observation, immunohistochemistry, and anatomical description) was made after careful observation of each injection site under microscope. Inclusion criteria were (a) having injection (i.e. syringe trace, damage, and the tracer) in amygdala and/or BNST nuclei; (b) having most of the tracer restricted in amygdala and BNST nuclei without much diffusion to other structures; and (c) consistency between injection nucleus and its already described projection patterns. For (c), literature was examined for known amygdala and BNST afferents. For instance, it is known that the CeA but not the BLA receives a dense projection from the BNST (Dong, Petrovich, Watts, & Swanson, 2001). Retrogradely labeled neurons in the BNST following injections to the BLA and the CeA were observed to confirm this pattern. BNST, on the other hand, receives afferents from the BLP and the centromedial amygdala but not much from the LA (Dong, Petrovich, & Swanson, 2001). Retrogradely labeled neurons in these amygdaloid nuclei following BNST injections were observed to confirm these projection patterns.

Surgeries were successful in 13 out of 16 cases (see Figure 5 for all injection sites). One case (animal RETT8) missed both the amygdala and the BNST targets. The rest of the cases (animals RETT1, RETT2, RETT3, RETT4, RETT5, RETT7, RETT9, RETT10, RETT11, RETT12, RETT13, RETT14) had successful injections

either in the amygdala (n = 8), the BNST (n = 12) or in both targets (n = 8). In animal RETT10, axonal transport of the Retrobeads was not successful following the injection to the amygdala, leaving seven successful amygdala injections. Of those, there were injections in the basolateral complex (n = 5) and injections in centromedial nuclei (n = 2). Basolateral complex injections consisted of injections to the LA, BLA, and BLP. Injections to all these nuclei will be referred to as BLA injections hereafter. Injections to the centromedial nuclei consisted of an injection to the CeA and an injection to the MeA which are pooled together due to the small number. They will be referred to as CeA and MeA injections hereafter (see Figure 6 for some of the amygdala injection sites). All BNST injections were in the central BNST, either anteriorly or posteriorly, with injections in lateral nuclei next to the internal capsule (n = 3), injections in medial nuclei (n = 6), and injections covering both medial, intermediate, and lateral nuclei (n = 3). BNST injections will be referred to as BNSTc injections hereafter to cover different target nuclei (see Figure 7 for some of the BNST injection sites).

According to inclusion criteria, three cases were approached with caution. In an amygdala injection (RETT13), tracer was diffused to the dorsal endopiriform nucleus (DEn) lateral to the amygdala. In two lateral BNST injections (RETT10 and RETT14), tracer was diffused to the internal capsule (ic). However, injections and most of the tracer were in the target amygdala and BNST nuclei. In these cases, literature was also examined to differentiate whether retrogradely labeled neurons in basal forebrain nuclei are due to injections to the amygdala and the BNST or due to the diffusion of tracers. In addition, there was a small amount of dorsal diffusion of tracers following each injection. This type of diffusion was due to the retrieval of injection syringe and was considered negligible.

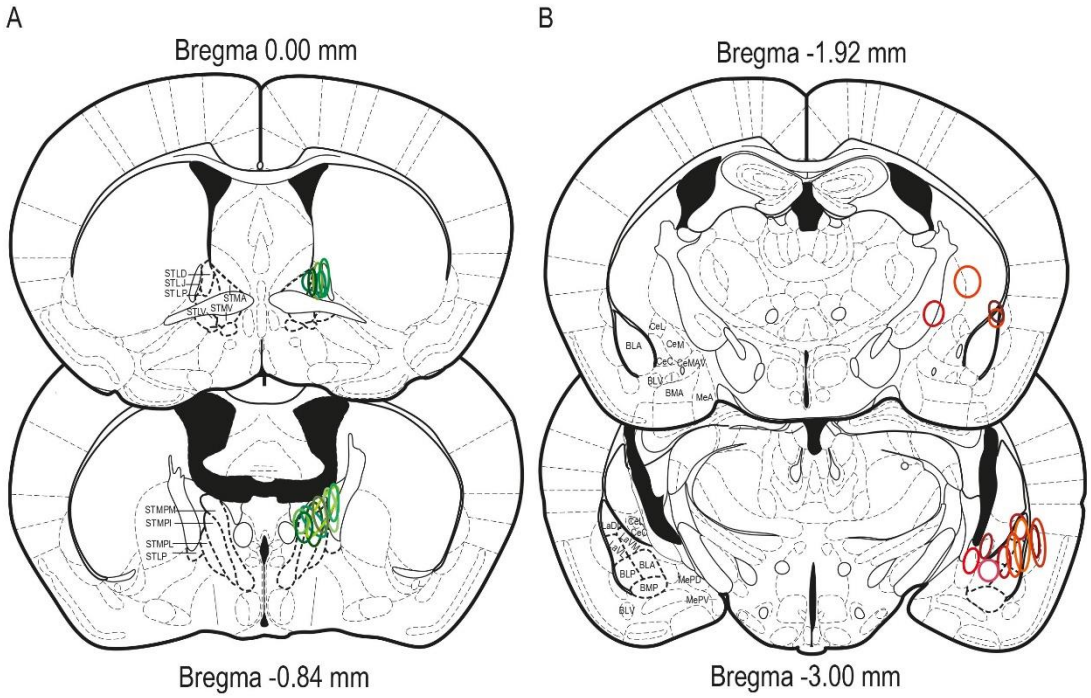

Fig. 5 All amygdala and BNST injection sites
Note: **A** All BNST injection sites in anterior (Bregma 0.00 mm) and posterior (Bregma -0.84 mm) BNST levels. On the left hemisphere, different BNST nuclei are demonstrated. On the right hemisphere, each ellipse with a different shade of green represents a BNST injection site. **B** All amygdala injection sites in anterior (Bregma -1.92 mm) and posterior (Bregma -3.00 mm) amygdala levels. On the left hemisphere, different amygdala nuclei are demonstrated. On the right hemisphere, each ellipse with a different shade of red represents an amygdala injection site. Note that injection hemispheres were counterbalanced and there were injections in the left hemisphere. However, here, all injections were plotted in the right hemisphere for demonstration purposes. Coronal maps are adapted from Paxinos and Franklin (2001). Refer to abbreviations

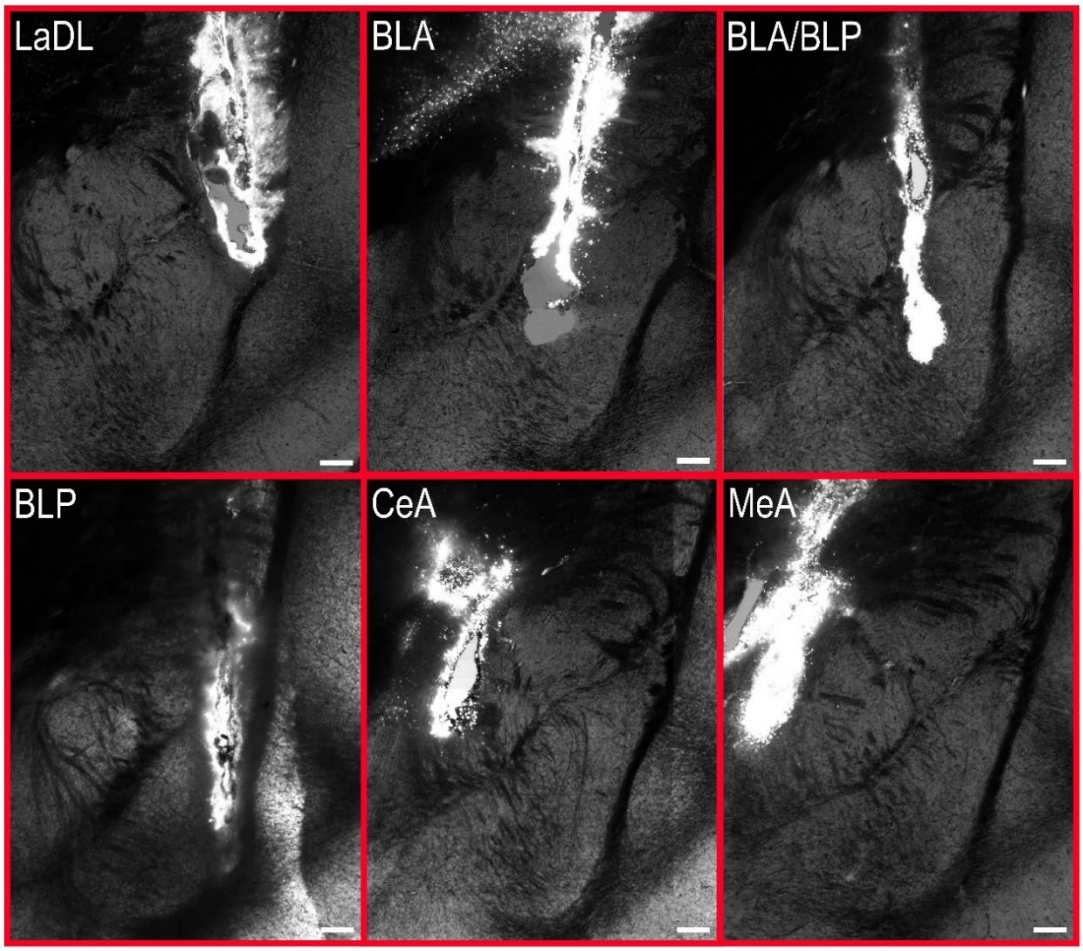

Fig. 6 Photomicrographs of amygdala injection sites
Note: Targeted amygdala nuclei are named on top left (refer to abbreviations). Scale bars: 200 μm

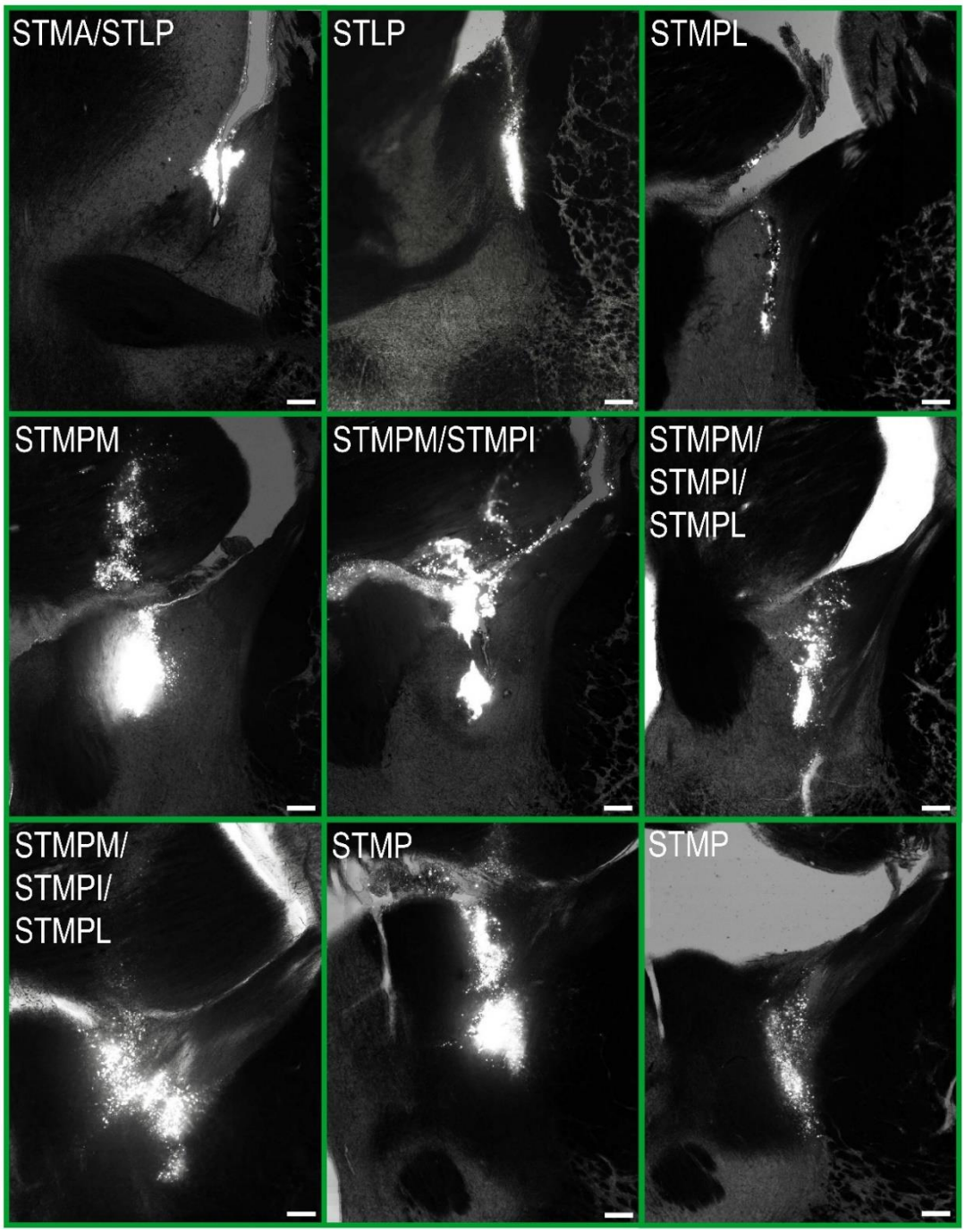

Fig. 7 Photomicrographs of BNST injection sites
Note: Targeted BNST nuclei are named on top left (refer to abbreviations). Scale bars: 200 μm

4.2 Retrograde tract-tracing results

4.2.1 Basal forebrain projections to the BLA

Injections to the basolateral amygdala (BLA) (n = 5) labeled neurons in basal forebrain nuclei, thalamic nuclei, hypothalamic nuclei including preoptic nuclei, the cerebral cortex, and the BNST in the basal forebrain levels observed (see Figure 8 for total number of labeled neurons in basal forebrain and preoptic nuclei).

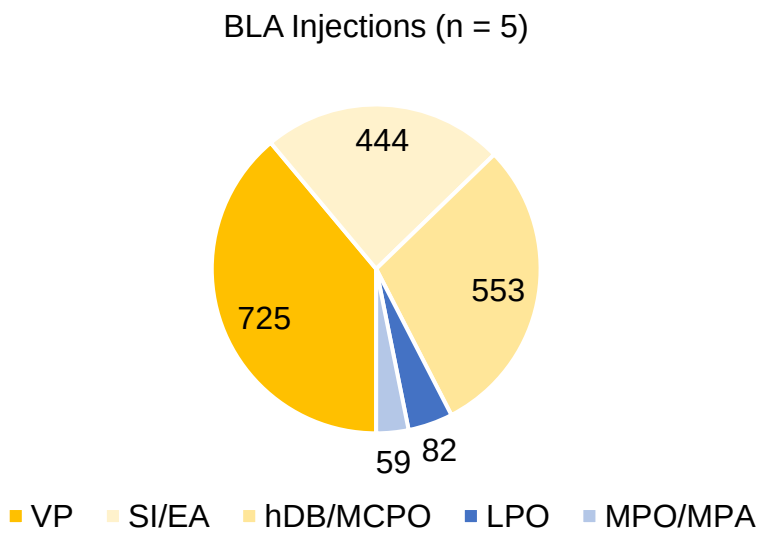

Fig. 8 Total number of labeled neurons in basal forebrain and preoptic nuclei following BLA injections

Confirming the existing literature (see Chapter 2), VP and SI/EA were the primary basal forebrain nuclei projecting to the BLA. There were also projections from the hDB/MCPO, to a lesser extent (Figure 9). LA and BLA/BLP injections differed in the number of neurons labeled. Injections confined only to the LA labeled less neurons in the VP, the SI/EA and the hDB/MCPO compared to BLA and BLP injections.

Anteriorly, labeled neurons were present in the VP and the hDB/MCPO with the VP giving rise to more projections. Labeled neurons were scattered across these nuclei without a preferential topography. However, group of neurons were observed in the VP close to the interstitial nucleus of the posterior limb of the anterior commissure, medial part (IPACM). Occasionally, a few neurons were observed in the MS/vDB but they were negligible in number. Posteriorly, in VP levels where it merges with central amygdaloid nucleus, medial part (CeM), a group of neurons was observed. There were more projecting neurons in ventral parts of the SI/EA compared to dorsal parts. There were also neurons scattered across the hDB/MCPO. Combined with the projections from the lateral preoptic area (LPO), medial preoptic nucleus (MPO), and medial preoptic area (MPA), 42% of the projecting neurons were located in the SI/EA followed by 26% in the VP, 16% in the hDB/MCPO, and 9% and 7% in the LPO and the MPO/MPA, respectively (see Figure 9).

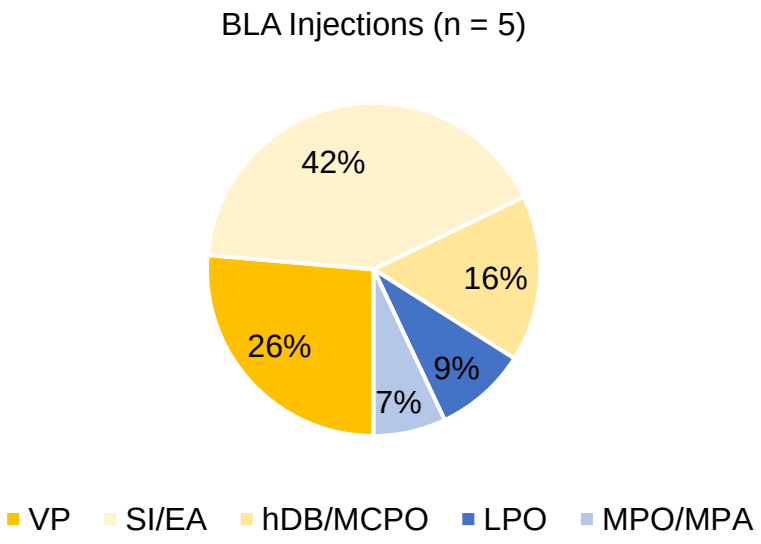

Fig. 9 Percentages of BLA-projecting basal forebrain and preoptic nuclei neurons
Note: Total number of neurons observed in each nucleus in each brain was normalized by division by the number of sections observed

4.2.2 Basal forebrain projections to the CeA and MeA

Injections to the centromedial amygdala (CeA and MeA) (n = 2) labeled more neurons in basal forebrain nuclei compared to BLA injections. The MeA injection also labeled more neurons compared to the CeA injection. However, there was only one injection to both structures and the data from both brains were pooled together (see Figure 10 for total number of labeled neurons in basal forebrain and preoptic nuclei).

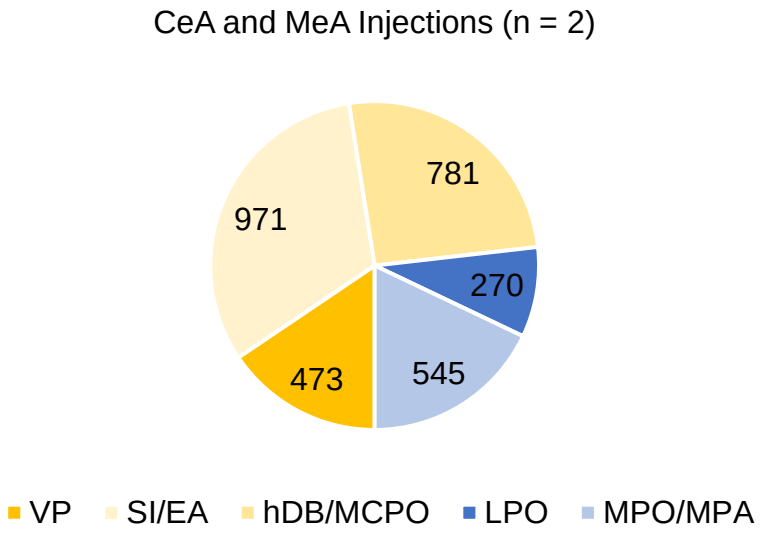

Fig. 10 Total number of labeled neurons in basal forebrain and preoptic nuclei following CeA and MeA injections

Following the CeA injection, anteriorly, there were not many labeled neurons in the VP and the hDB/MCPO. Many labeled neurons were located in the lateral BNST. In contrast to BLA injections, there were also many neurons in preoptic nuclei. More posteriorly, there were less labeled neurons in BNST and preoptic nuclei but more labeled neurons in the VP/SI/EA and the hDB/MCPO. In addition,

labeling was observed in the supraoptic nucleus (SO), the anterior hypothalamic area, anterior part (AHA), and the peduncular part of lateral hypothalamus (PLH).

Following the MeA injection, there was heavy labeling in amygdala nuclei, thalamic nuclei, hypothalamic nuclei including preoptic nuclei, and the BNST. Anteriorly, many labeled neurons were observed in the BNST. The majority was located in lateral BNST nuclei but many labeled neurons were also observed in medial BNST nuclei in more anterior levels. Among basal forebrain nuclei, more labeled neurons were observed in the hDB/MCPO and the SI compared to the VP. Interestingly, in contrast to BLA injections, many labeled neurons were also present in the MS/vDB. Posteriorly, more neurons were observed in the SI/EA and the hDB/MCPO compared to the VP. The MeA, the paratenial thalamic nucleus (PT), the paraventricular thalamic nucleus, anterior part (PVA), and the anteromedial thalamic nucleus (AM) also gave rise to heavy projections together with basal forebrain nuclei. Not as many labeled neurons were present in BNST and preoptic nuclei compared to those in amygdala nuclei, basal forebrain nuclei, and thalamic nuclei. More posteriorly, even more neurons were observed in the SI/EA, the hDB/MCPO, and amygdala nuclei while those in thalamic, BNST, and preoptic nuclei decreased in number. Labeled neurons were also observed in the retrochiasmatic area. Combined with the projections from the LPO, the MPO, and the MPA, the SI/EA gave rise to 43% of projections to the CeA and MeA followed by 15% from the hDB/MCPO, 13% from the VP, and 17% and 12% from the MPO/MPA and the LPO, respectively (see Figure 11).

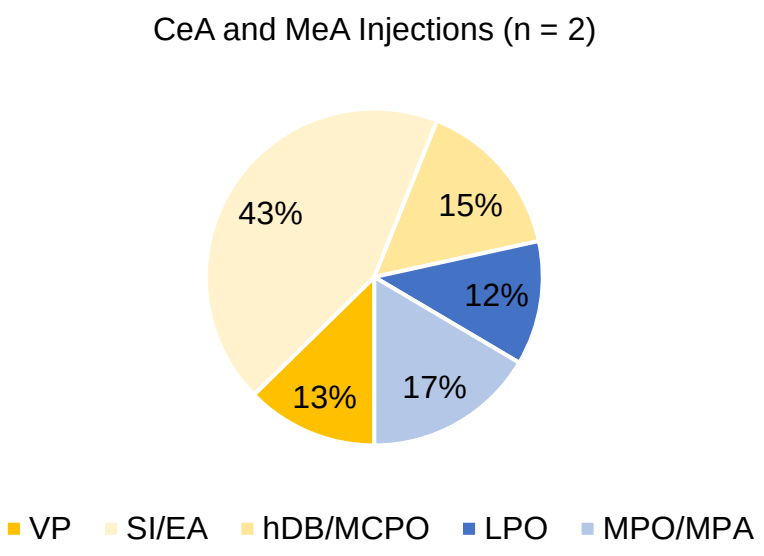

Fig. 11 Percentages of CeA- and MeA-projecting basal forebrain and preoptic nuclei neurons
Note: Total number of neurons observed in each nucleus in each brain was normalized by division by the number of sections observed

4.2.3 Basal forebrain projections to the BNSTc

In basal forebrain levels observed, BNST injections (n = 12) invariably labeled neurons in preoptic nuclei. This pattern was observed along the rostrocaudal extent and irrespective of the injection nuclei. Labeled neurons were observed in the MPA, medial and lateral parts of the MPO (MPOM and MPOL, respectively), and the ventrolateral preoptic nucleus (VLPO). Labeled neurons were also present in the LPO, to a lesser extent. In basal forebrain nuclei, anteriorly, there were few labeled neurons in the VP. The hDB/MCPO gave rise to more projecting neurons compared to the VP. However, they were not so numerous, either. Posteriorly, labeled neurons were observed in hypothalamic nuclei, including preoptic nuclei and the PLH. Similar to anterior levels, the VP gave rise to a small number of projecting neurons. However, labeled neurons were observed in the SI/EA and the hDB/MCPO (see

Figure 12 for total number of labeled neurons in basal forebrain and preoptic nuclei). In the SI/EA, labeled neurons were preferentially located in dorsal parts compared to ventral parts. Overall, combined with the projections from the LPO, the MPO, and the MPA, 46% of the projecting neurons were located in the MPO/MPA followed by 21% in the SI/EA, 14% in the LPO, 13% in the hDB/MCPO, and 6% in the VP (Figure 13).

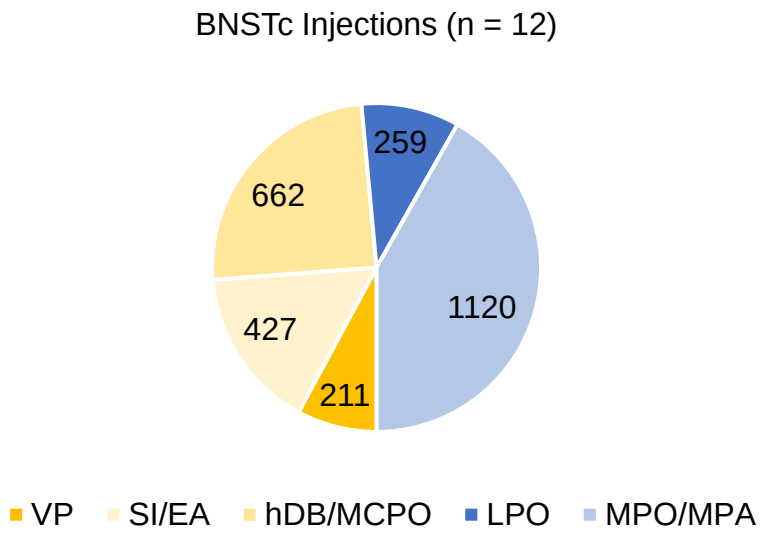

Fig. 12 Total number of labeled neurons in basal forebrain and preoptic nuclei following BNSTc injections

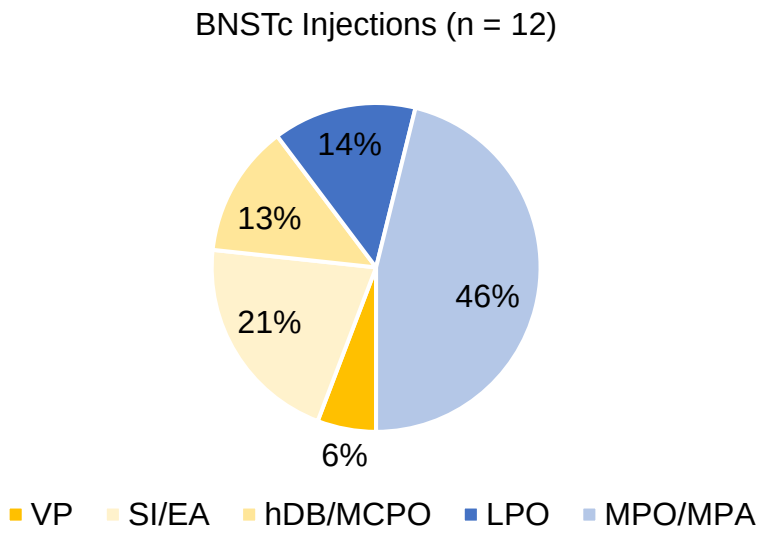

Fig. 13 Percentages of BNSTc-projecting basal forebrain and preoptic nuclei neurons
Note: Total number of neurons observed in each nucleus in each brain was normalized by division by the number of sections observed

4.2.4 Basal forebrain projections to both the amygdala and the BNST

In all the brains observed, basal forebrain neurons projecting both to the amygdala and the BNST were not encountered except for two neurons double-labeled with red and green beads in the hDB/MCPO in animal RETT12. However, in some cases, separate neurons labeled with red and green beads were in close proximity in the same basal forebrain nuclei (Figure 14). Although whether amygdala- and BNST-projecting basal forebrain neurons form synapses is beyond the scope of this study, this can be likely considering their proximity.

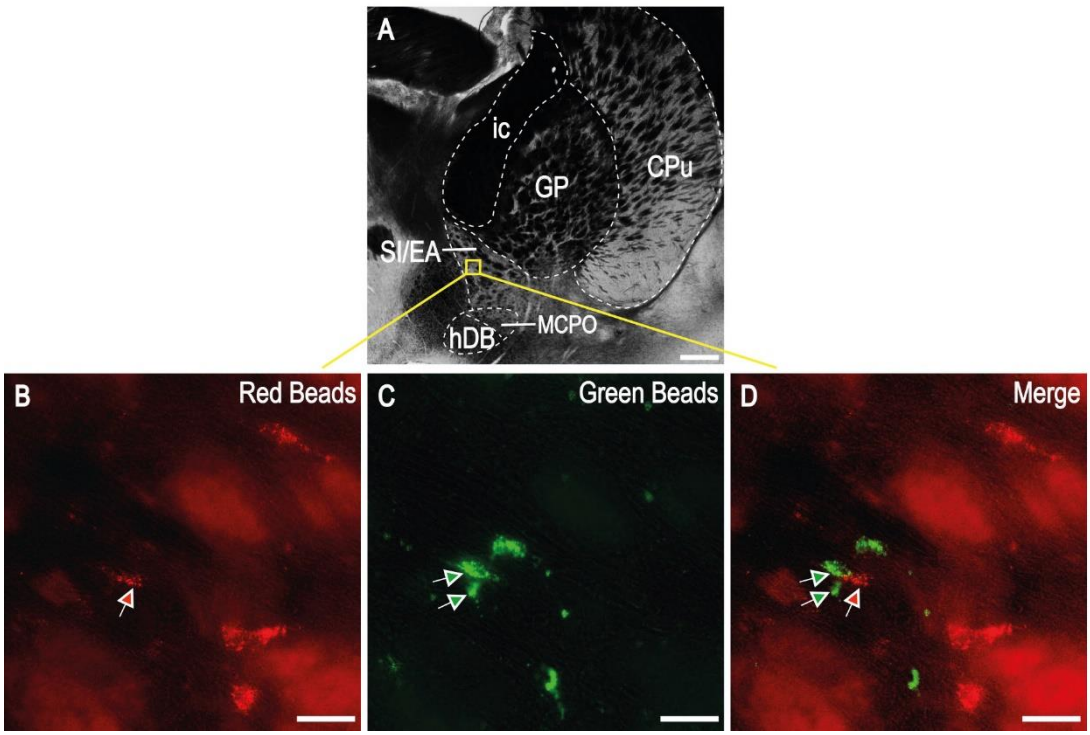

Fig. 14 Amygdala- and BNST-projecting neurons are closely located
Note: Red and green Retrobeads injections to the amygdala and the BNST labeled neurons in the SI/EA in animal RETT12. **A** A region was marked with a yellow square in the SI/EA. **B-D** Magnified versions of the square in **(A)**. **B** Red beads labeled neurons; **C** Green beads labeled neurons; **D** Merge. Note that the neurons pointed with arrows are closely located. Scale bars: **A** 500 μm, **B-D** 50 μm. Refer to abbreviations

4.3 Immunohistochemistry results

27 brain sections from basal forebrain levels were used for calbindin (CB), parvalbumin (PV), and special AT-rich sequence-binding protein-1 (SATB1) immunohistochemistry staining. Sections used were taken from nine brains expressing high numbers of retrogradely labeled neurons. Sections were selected such that both anterior and posterior basal forebrain levels were taken. Leu-enkephalin labeling was not included here. As mentioned above, leu-enkephalin labels fibers and it was not used to count cell bodies, but as a regional marker for the VP (Figure 15).

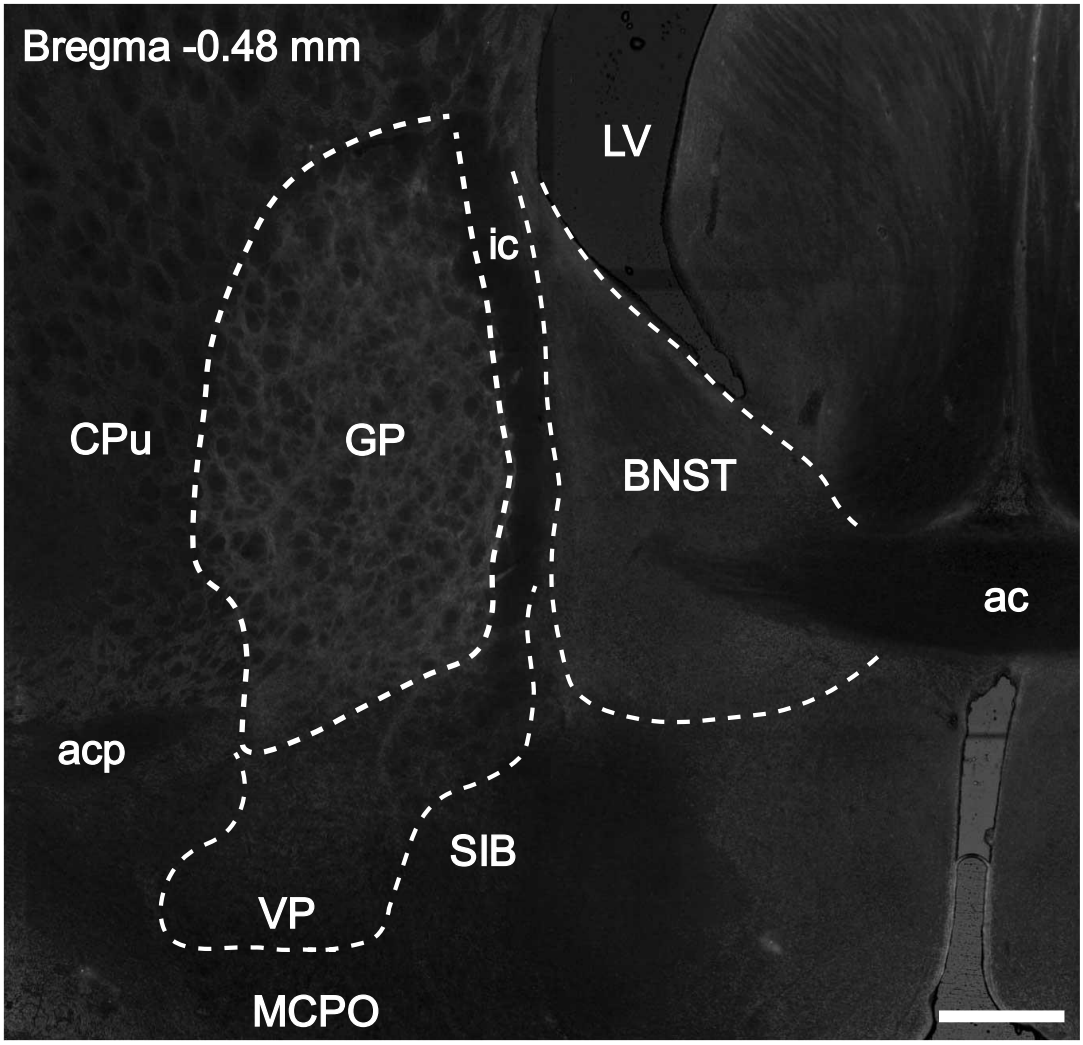

Fig. 15 Leu-enkephalin as a regional marker for the VP
Note: Leu-enkephalin labeled fibers in pallidal regions (GP and VP) mark the borders of these regions. Note the lighter-looking appearance of the GP and the VP due to labeled fibers compared to neighboring structures. Labeled fibers are also observed in lateral BNST nuclei medial to the ic. Scale bar 500 μm. Refer to abbreviations

4.3.1 CB and PV labeling for BLA-projecting basal forebrain neurons

Six sections from three different brains were labeled for CB. Three of them were from anterior basal forebrain levels and the other three were from posterior basal forebrain levels. Anteriorly, the highest number of CB-immunopositive neurons were observed in the VP, followed by the hDB/MCPO and the SI. More posteriorly, in

small VP levels, more neurons were observed in the SI/EA compared to the VP. CB-immunopositive neurons were scattered in the dorsal SI/EA. Groups of neurons were also located in the ventral SI/EA, ventral to the GP and the CPu border. Overall, there was not a heavy CB labeling in basal forebrain nuclei. However, in all basal forebrain nuclei, CB-immunopositive cell bodies outnumbered retrogradely labeled cell bodies. Number of cell bodies single- and double-labeled for beads and CB in all basal forebrain nuclei were pooled. This showed that 2% of the neurons (n = 9) were double-labeled for beads and CB (Figure 16). Looking at basal forebrain nuclei separately revealed that the highest number of CB-immunopositive cell bodies were located in the SI/EA followed by the hDB/MCPO and the VP. Same pattern was observed for retrogradely labeled neurons. However, there was no double-labeled neurons in the SI/EA. Eight of the double-labeled neurons were observed in the VP (see Figure 18 for a coronal map of the VP with double-labeled neurons) and one of them was observed in the hDB/MCPO (Figure 17).

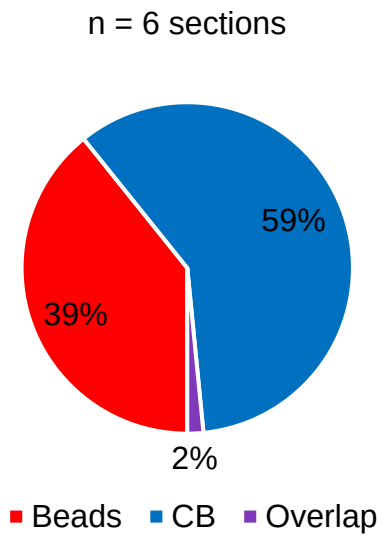

Fig. 16 Percentages of beads and CB single- and double-labeling following BLA injections
Note: Observed numbers in all basal forebrain nuclei are pooled

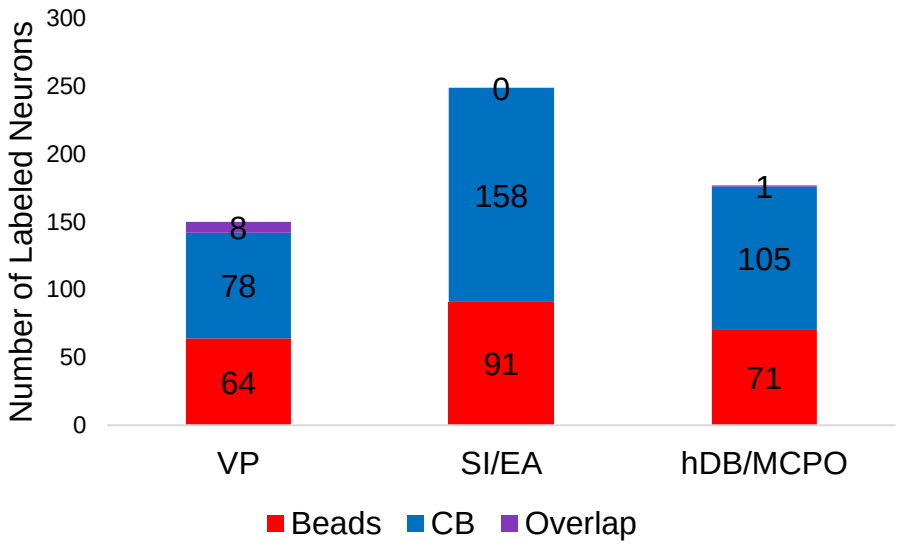

Fig. 17 Number of beads and CB single- and double-labeled neurons in basal forebrain nuclei following BLA injections

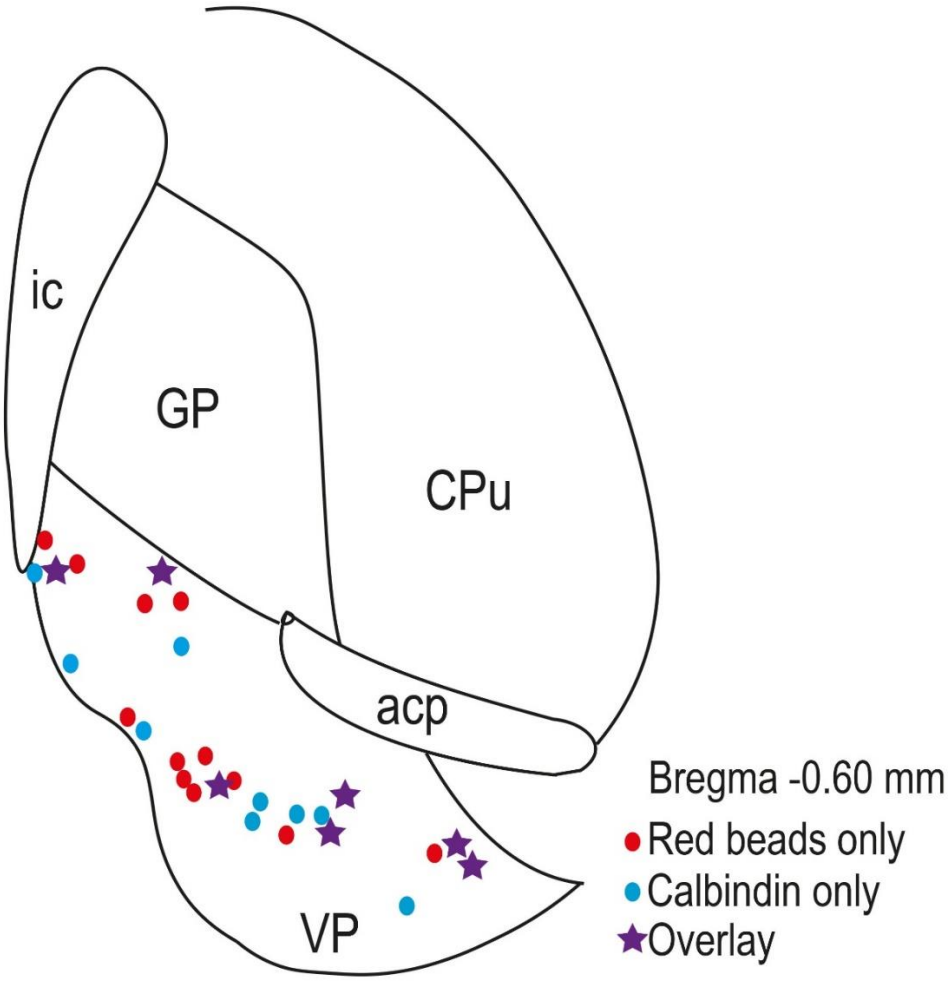

Fig. 18 Coronal map of beads and CB labeling in the VP in animal RETT7
Note: In animal RETT7, red Retrobeads was injected to the BLA/BLP. Retrogradely labeled neurons (red circles) were observed in the VP. Later CB immunostaining revealed both single- (blue circles) and double-labeled (purple stars) neurons. Double-labeled neurons were mostly located in ventral parts of the VP. Coronal map was adapted from Paxinos and Franklin (2001). Refer to abbreviations

Five sections from three different brains were labeled for PV. Three of them were from anterior basal forebrain levels while the other two were from posterior basal forebrain levels. PV-immunopositive neurons in basal forebrain nuclei were less numerous compared to CB-immunopositive neurons. Anteriorly, the highest number of PV-immunopositive neurons were located in the VP followed by the hDB/MCPO and the SI. Posteriorly, they were preferentially located in the ventral SI/EA close to the VP compared to the dorsal SI/EA. They were also outnumbered

by retrogradely labeled neurons in each basal forebrain nucleus. Number of cell bodies single- and double-labeled for beads and PV in all basal forebrain nuclei were pooled. This showed that 2% of the neurons (n = 5) were double-labeled for beads and PV (Figure 19). Overall, the highest number of PV-immunopositive neurons were observed in the VP followed by the hDB/MCPO and the SI/EA. All of the double-labeled neurons were located in the VP (Figure 20).

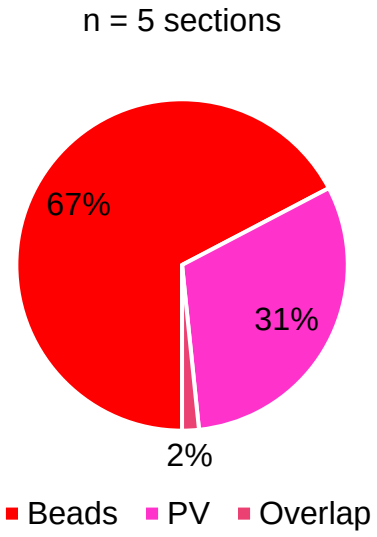

Fig. 19 Percentages of beads and PV single- and double-labeling following BLA injections
Note: Observed numbers in all basal forebrain nuclei are pooled

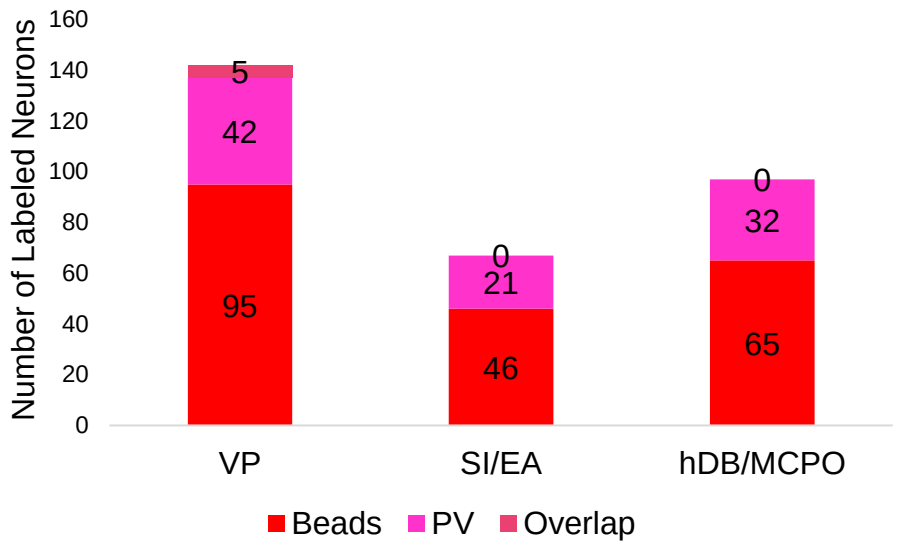

Fig. 20 Number of beads and PV single- and double-labeled neurons in basal forebrain nuclei following BLA injections

4.3.2 CB and PV labeling for CeA- and MeA-projecting basal forebrain neurons

Three sections from two CeA and MeA injection brains were labeled for CB (n = 1 from the CeA, n = 2 from the MeA). Two of the sections were from posterior basal forebrain levels at which the VP no longer existed. CB-immunopositive neurons showed similar distribution patterns in basal forebrain nuclei as detailed above. In contrast to BLA injections, however, cell bodies labeled with beads outnumbered CB-immunopositive cell bodies. Pooling all labeled neurons in all basal forebrain nuclei revealed double-labeling in 4% of the neurons (n = 24) (Figure 21). Most of the single labeled neurons were located in the SI/EA where most of the double-labeled neurons were also located (n = 18) (see Figure 23 for a coronal map of the SI/EA with double-labeled neurons and Figure 24 for photomicrographs of beads and CB single- and double-labeled neurons in the SI/EA). However, double-labeled

neurons were also encountered in the VP (n = 4) and the hDB/MCPO (n = 2) (Figure 22).

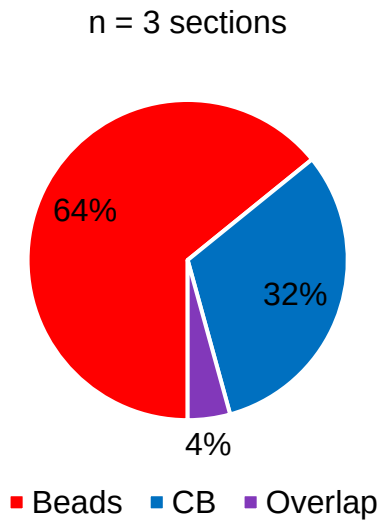

Fig. 21 Percentages of beads and CB single- and double-labeling following CeA and MeA injections
Note: Observed numbers in all basal forebrain nuclei are pooled

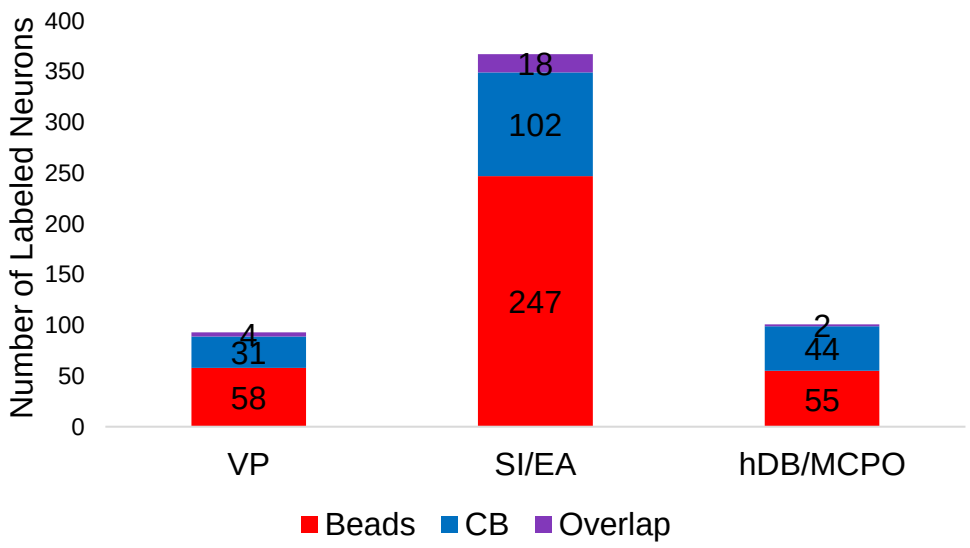

Fig. 22 Number of beads and CB single- and double-labeled neurons in basal forebrain nuclei following CeA and MeA injections

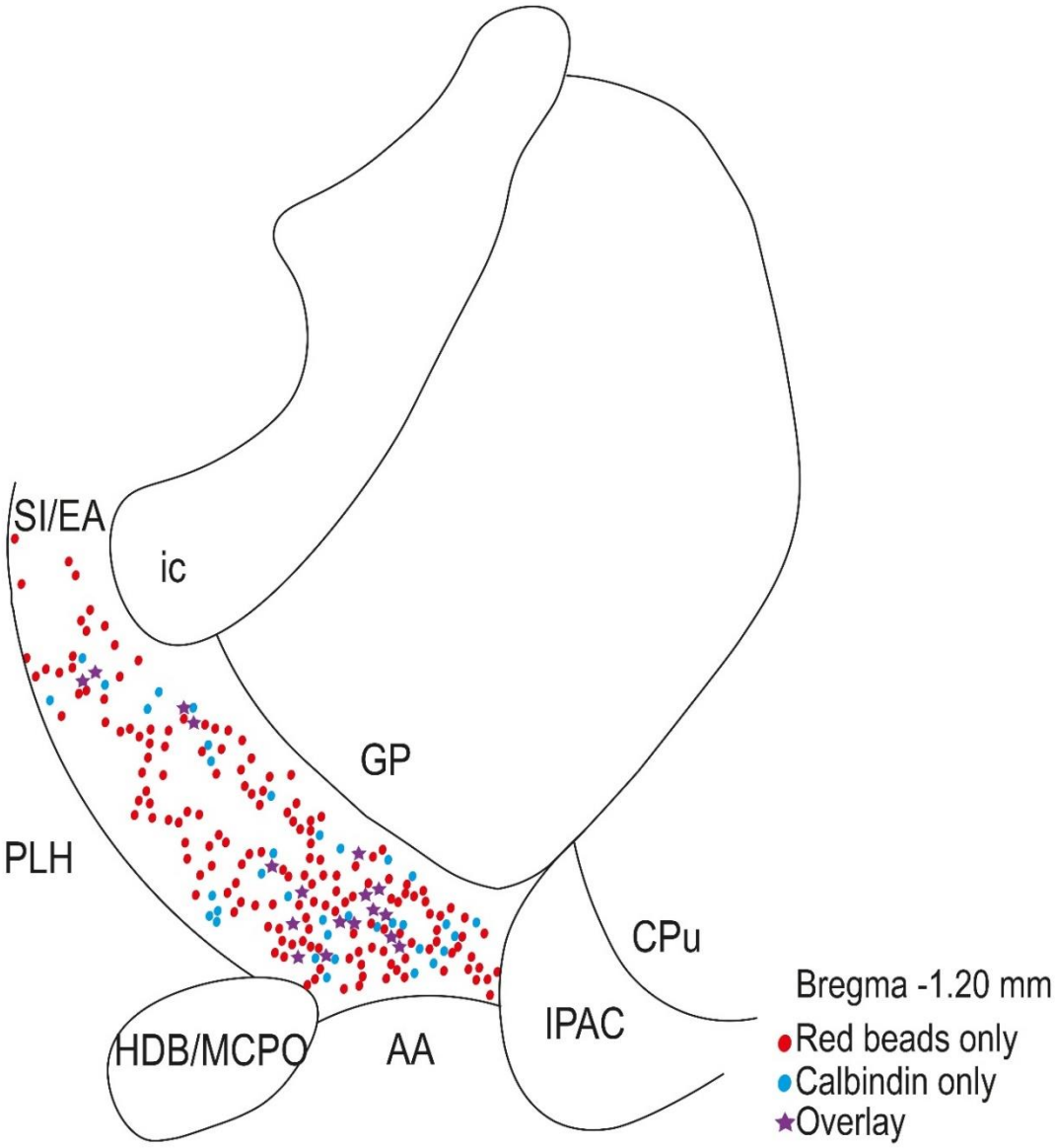

Fig. 23 Coronal map of beads and CB labeling in the SI/EA in animal RETT11
Note: In animal RETT11, red Retrobeads was injected to the MeA. Retrogradely labeled neurons (red circles) were observed in the SI/EA. Later CB immunostaining revealed both single- (blue circles) and double-labeled (purple stars) neurons. Double-labeled neurons were mostly located in ventral parts of the SI/EA. Coronal map was adapted from Paxinos and Franklin (2001). Refer to abbreviations

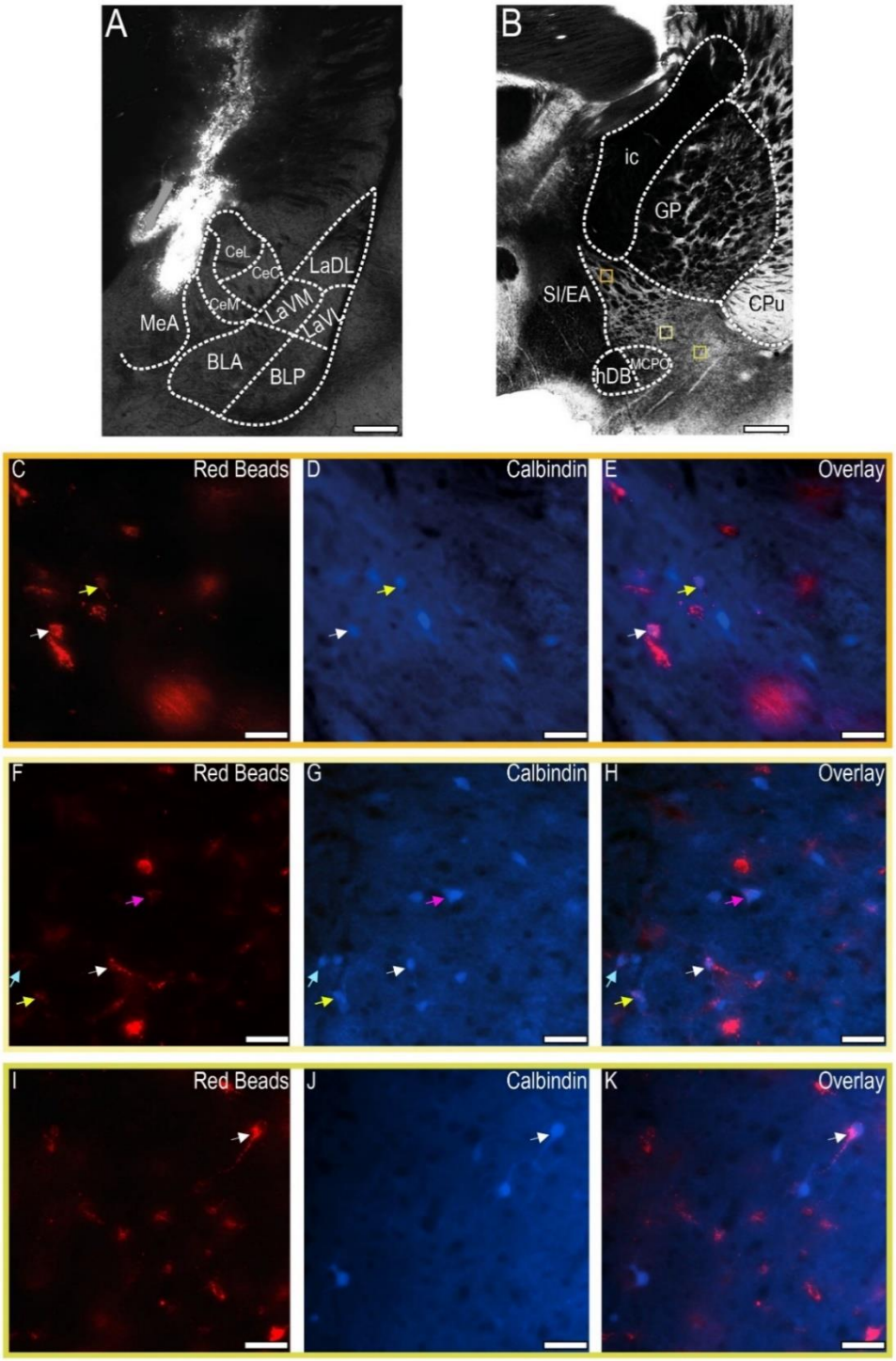

Fig. 24 Photomicrographs of beads-CB double-labeled neurons in the SI/EA
Note: **A** Red Retrobeads injection to the MeA in animal RETT11 labeled neurons in basal forebrain nuclei. **B** Many retrogradely labeled neurons as well as CB-immunopositive neurons were observed in the SI/EA at the Bregma level -1.20 mm. Three SI/EA regions with beads-CB double-labeled neurons were marked with squares with different shades of yellow. **C-E**, **F-H**, **I-K** Magnified versions of the squares in **(B)**. **C**, **F**, **I** Red beads labeled neurons; **D**, **G**, **J** CB-immunopositive neurons; **E**, **H**, **K** Overlap. Note that the arrows point double-labeled neurons. Scale bars: **A**, **B** 500 μm; **C-K** 50 μm. Refer to abbreviations

Three other sections from the CeA and MeA injection brains were labeled for PV (n = 1 from the CeA, n = 2 from the MeA). One section was from a posterior basal forebrain level at which the VP no longer existed. PV-immunopositive neurons showed similar distribution patterns in basal forebrain nuclei as detailed above. They were similarly outnumbered by neurons labeled with beads in all basal forebrain nuclei. Pooling all basal forebrain nuclei revealed double-labeling in 1% of the neurons (n = 3) (Figure 25). Two of the double-labeled neurons were located in the SI/EA where most of the neurons labeled with beads were also located. One double-labeled neuron was encountered in the hDB/MCPO which showed the lowest number of neurons labeled with beads and PV (Figure 26).

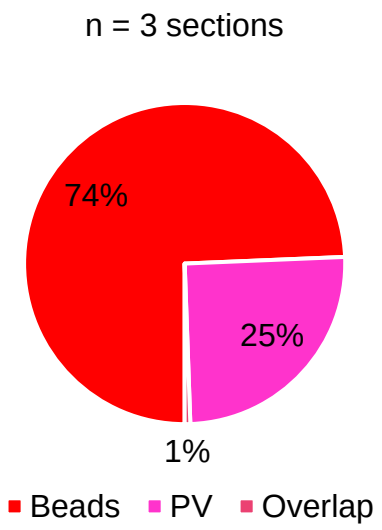

Fig. 25 Percentages of beads and PV single- and double-labeling following CeA and MeA injections
Note: Observed numbers in all basal forebrain nuclei are pooled

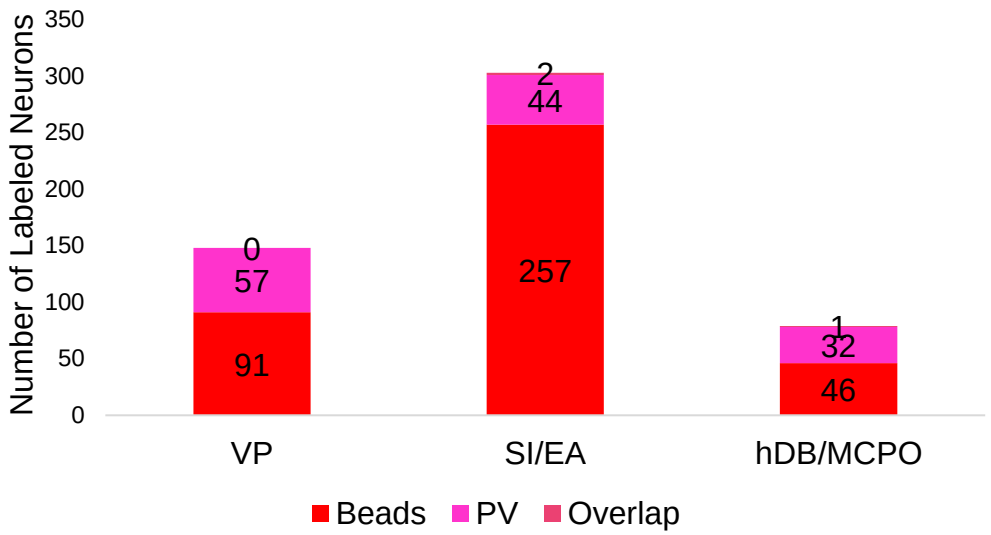

Fig. 26 Number of beads and PV single- and double-labeled neurons in basal forebrain nuclei following CeA and MeA injections

4.3.3 CB, PV, and SATB1 labeling for BNSTc-projecting basal forebrain neurons

Nine sections from six different brains with BNSTc injections were labeled for CB. Five sections were from posterior basal forebrain levels at which the VP no longer existed. CB-immunopositive neurons showed similar distribution patterns in basal forebrain nuclei as detailed above. Importantly, in the SI/EA, they were located in ventral portions. Neurons labeled with beads, on the other hand, were located mostly in dorsal and middle portions of the SI/EA. There were more CB-immunopositive neurons compared to neurons labeled with beads in each basal forebrain nucleus. Pooling all neurons labeled for beads and CB in all basal forebrain nuclei revealed that 1% (n = 7) of the neurons were double-labeled (Figure 27). Six of the double-labeled neurons were located in the SI/EA where the highest number of beads and CB labeled neurons were also located. In addition, one double-labeled neuron was observed in the hDB/MCPO (Figure 28).

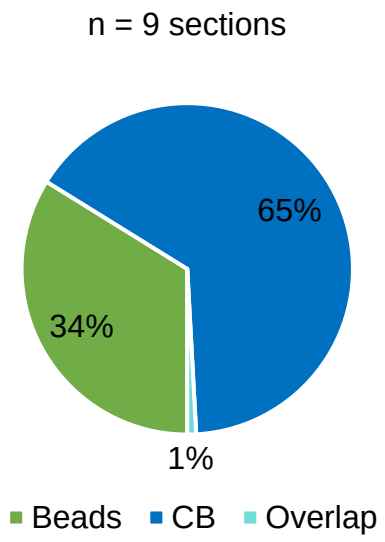

Fig. 27 Percentages of beads and CB single- and double-labeling following BNSTc injections
Note: Observed numbers in all basal forebrain nuclei are pooled

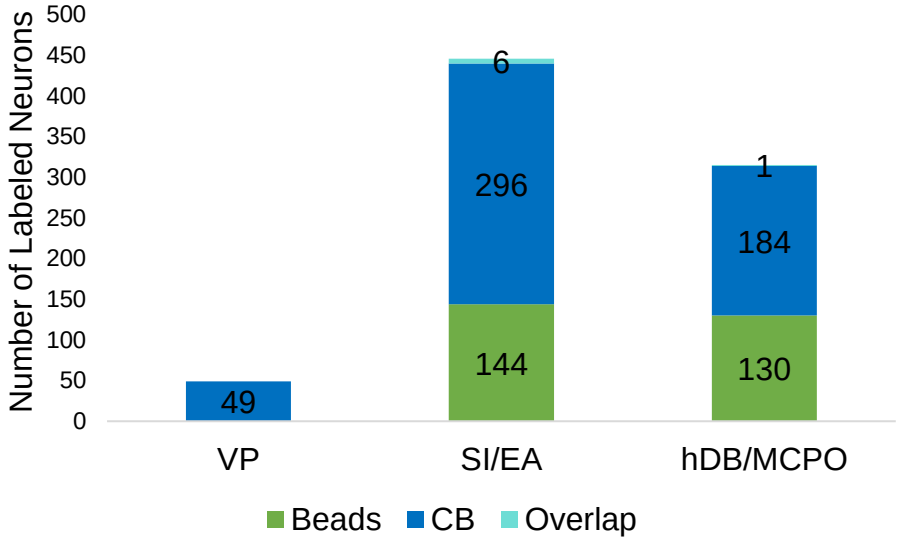

Fig. 28 Number of beads and CB single- and double-labeled neurons in basal forebrain nuclei following BNSTc injections
Note: Retrogradely labeled and double-labeled (overlap) neurons were not observed in the VP in these nine sections

Eight sections from six different brains with BNSTc injections were labeled for PV. PV-immunopositive neurons showed similar distribution patterns in basal forebrain nuclei as detailed above. In the SI/EA, while PV-immunopositive neurons were mostly located in ventral parts, neurons labeled with beads were more numerous in dorsal parts. Similar to the labeling results for BLA and CeA and MeA, PV labeled less neurons in basal forebrain nuclei compared to CB. Combining labeled neurons in all basal forebrain nuclei resulted in the same number of beads and PV labeled neurons. Each group constituted 50% of the neurons with zero overlap (Figure 29). That is, no double-labeled neurons were observed in any of the basal forebrain nuclei (Figure 30).

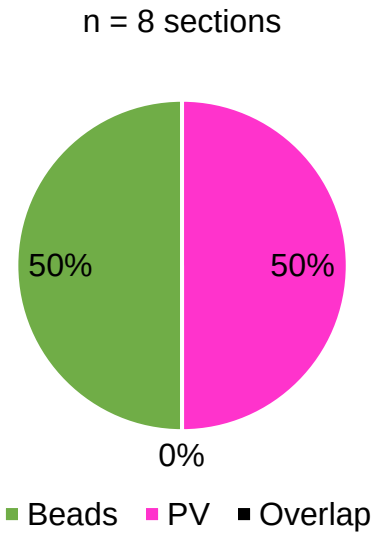

Fig. 29 Percentages of beads and PV single- and double-labeling following BNSTc injections
Note: Observed numbers in all basal forebrain nuclei are pooled

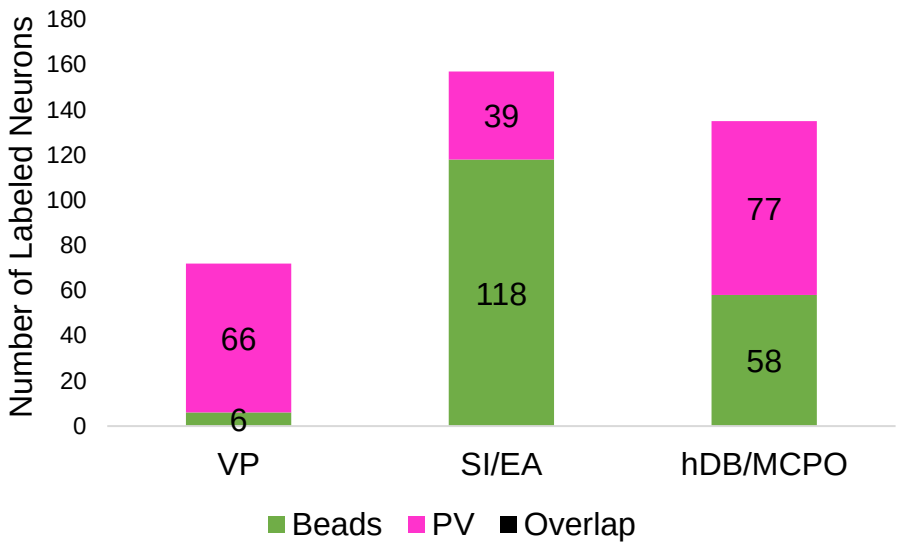

Fig. 30 Number of beads and PV single- and double-labeled neurons in basal forebrain nuclei following BNSTc injections
Note: No beads-PV double-labeling (overlap) was observed in basal forebrain nuclei

Three additional sections from a brain with BNSTc injection were labeled for SATB1. Both anteriorly and posteriorly, SATB1-immunopositive neurons were preferentially located in ventral basal forebrain. Those in the VP were located near the GP border. Many were observed in the hDB/MCPO which outnumbered neurons labeled with beads. SATB1-immunopositive hDB/MCPO neurons also outnumbered those SATB1-immunopositive neurons in the VP and the SI/EA. When pooled together with neurons labeled with beads in all basal forebrain nuclei, SATB1-immunopositive neurons constituted the majority with 79% (Figure 31). In the hDB/MCPO, neurons labeled with beads were located in dorsal portions while those labeled with SATB1 were located in ventral portions. Although some SATB1-immunopositive neurons were closely located to neurons labeled with beads, no double-labeling was observed in any of the basal forebrain nuclei (Figure 32).

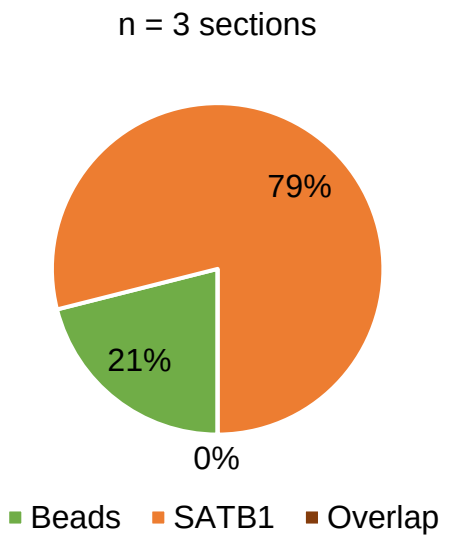

Fig. 31 Percentages of beads and SATB1 single- and double-labeling following BNSTc injections
Note: Observed numbers in all basal forebrain nuclei are pooled

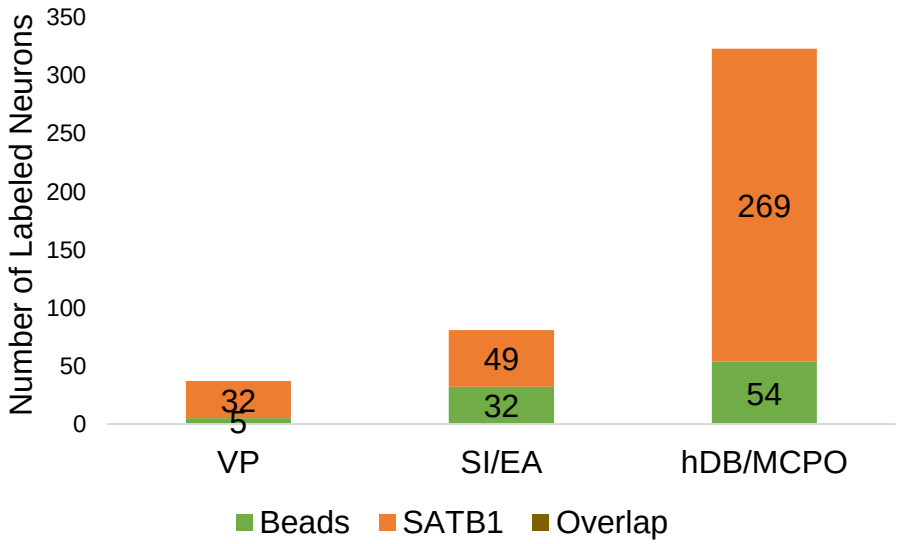

Fig. 32 Number of beads and SATB1 single- and double-labeled neurons in basal forebrain nuclei following BNSTc injections
Note: No beads-SATB1 double-labeling (overlap) was observed in basal forebrain nuclei

CHAPTER 5

DISCUSSION

This study aimed at describing basal forebrain GABAergic projections to the amygdala and the BNST. Microinjections of the retrograde tracer Retrobeads to these structures labeled many neurons. Those in basal forebrain nuclei were examined thoroughly. Immunohistochemical staining revealed some of the putative GABAergic subgroups among the projecting neurons. Supporting earlier findings, PV-immunopositive neurons in several basal forebrain nuclei projected to the amygdala (Do et al., 2016; Mascagni & McDonald, 2009). More importantly, this study showed for the first time that CB-immunopositive neurons in basal forebrain nuclei also project to the basolateral amygdala, centromedial amygdala, and the BNST.

Retrobeads injections to the BLA labeled the highest number of neurons in the SI/EA followed by the VP and the hDB/MCPO. Subsequent CB labeling also revealed neurons in these nuclei which outnumbered retrogradely labeled neurons. Cell body counting in immunohistochemistry sections revealed the highest number of retrogradely-labeled and CB-immunopositive neurons in the SI/EA followed by the hDB/MCPO and the VP. However, almost all of the beads-CB double-labeled neurons were located in the VP except for one neuron in the hDB/MCPO. PV did not label as many neurons in basal forebrain nuclei compared to CB and PV-immunopositive neurons were outnumbered by retrogradely-labeled neurons. Majority of the beads and PV single-labeled neurons were located in the VP. All of the beads-PV double-labeled neurons were also observed in the VP.

Retrobeads injections to the centromedial amygdaloid nuclei CeA and MeA labeled many neurons in the same basal forebrain nuclei. The SI/EA gave rise to majority of the projections followed by the hDB/MCPO and the VP. CB labeled neurons in these nuclei were outnumbered by retrogradely labeled neurons. Most of the CB single-labeled neurons were observed in the SI/EA where most of the beads-CB double-labeled neurons were also located. However, double-labeling was also observed in the VP and the hDB/MCPO to a lesser extent. Similar to BLA observations, PV labeled fewer neurons in these nuclei compared to CB. In addition, PV-immunopositive neurons were outnumbered by retrogradely labeled neurons. Beads-PV double-labeled neurons were also less in number and were observed in the SI/EA and the hDB/MCPO but not in the VP.

Retrobeads injection to the BNSTc revealed that the BNST does not receive as many projections from the basal forebrain as the BLA and the CeA and MeA. More projections were originated from preoptic nuclei of the hypothalamus. Among the basal forebrain nuclei, the SI/EA contributed the most with the highest number of retrogradely labeled neurons. This was followed by the hDB/MCPO with the VP contributing the least. CB-immunopositive neurons outnumbered retrogradely labeled neurons in these nuclei. The highest number of beads and CB single-labeled neurons were observed in the SI/EA followed by the hDB/MCPO in which beads-CB double-labeling was also observed. Majority of the double-labeled neurons were located in the SI/EA with one neuron observed in the hDB/MCPO. PV and SATB1 also labeled neurons in basal forebrain nuclei. PV-immunopositive neurons were mostly located in the hDB/MCPO and the VP while SATB1-immunopositive neurons were mostly located in the hDB/MCPO. However, no beads-PV and beads-SATB1 double-labeling were observed in basal forebrain nuclei.

These results suggest that there are putative GABAergic subpopulations in basal forebrain nuclei projecting to the BLA, the CeA and MeA, and the BNST. CB- and PV-immunopositive BLA-projecting neurons were observed in the VP. In addition, a potential CB-immunopositive group is also located in the hDB/MCPO. CB-immunopositive CeA- and MeA-projecting neurons were observed mostly in the SI/EA although some were also present in the VP and the hDB/MCPO. PV-immunopositive neurons, on the other hand, seem to project less to the CeA and MeA compared to CB-immunopositive ones. This GABAergic subpopulation was observed in the SI/EA and the hDB/MCPO. Finally, there seems to be a CB-immunopositive putative GABAergic subpopulation in the SI/EA projecting to the BNST.

Basal forebrain nuclei classification used in this study was adapted from Paxinos and Watson (2007). However, a few points regarding the use of the nomenclature need to be clarified. hDB and MCPO are two nuclei next to each other (see Figure 3). In this study, cell counts were made in these structures as a whole and the two are referred to as hDB/MCPO. SI, anteriorly, was taken as the area between the dorsal part of the VP and the hDB. Posteriorly, nuclei named as sublenticular extended amygdala, central part (EAC) and medial part (EAM) in Paxinos and Watson (2007) together with the SI were named as SI/EA as the sublenticular extended amygdala is recognized as a part of the SI (Alheid & Heimer, 1988).

Interstitial nucleus of the posterior limb of the anterior commissure (IPAC), located ventral to the CPu in the rat brain, is another region recognized as a part of the basal forebrain (de Olmos, 1972; Gärtner, Härtig, Riedel, Brauer, & Arendt, 2002). It corresponds to the region known as the fundus striati in the human brain (Alheid & Heimer, 1988). However, the name fundus striati is also used for the rat

brain (Mascagni & McDonald, 2009). Mascagni and McDonald (2009) reported retrogradely labeled neurons in the fundus striati following Fluorogold injections to the basolateral complex. Some of these neurons were PV- or GAD-immunopositive GABAergic neurons. IPAC and the fundus striati were originally regarded as a ventral extension of the striatal system. However, IPAC is divided into medial (IPACM) and lateral (IPACL) portions which seem to differ in their connections and functions. While IPACM is more closely associated with the extended amygdala system, IPACL is more closely associated with the striatal system (Alheid & Heimer, 1996; Gärtner et al., 2002; Shammah-Lagnado, Alheid, & Heimer, 2001). In this study, both retrogradely and immunohistochemically labeled neurons were observed in the broad region that corresponds to the VP, IPACM, and the ventral SI/EA. However, IPACM was not included to the results as a separate basal forebrain nucleus. Posteriorly, VP and SI/EA regions used for cell counts did not include IPACM in all its mediolateral extent. Specifically, more lateral regions extending to the amygdaloid nuclei and the piriform cortex were excluded even though labeled neurons were observed. More posteriorly, starting approximately from the Bregma −1.44 mm level, IPACM gets smaller and it merges with the CeM. Many retrogradely labeled neurons were observed in this region. They were not included to cell counts, either, as this region was taken as the amygdala but not the basal forebrain. Not to confuse the SI/EA with the CeM, cell counts did not exceed Bregma -1.44 mm level. Therefore, cell counts presented in this study may be underestimations of the real numbers for not including the IPACM in its entirety and not including basal forebrain levels as far as the SI/EA continues.

Basal forebrain nuclei classifications in some of the previous tracing studies differ. For instance, Agostinelli et al. (2019) includes the VP in their classification of

the SI. However, closely examining the regions described in these studies reveal similar findings. Ottersen (1980) described cases RV4 and RV8 with HRP injections in the BLA. HRP was also taken by the BLP. These injections revealed retrogradely labeled neurons in the VP and the SI. RETT1 and RETT7 in this study are similar to RV4 and RV8. Consistently, retrogradely labeled neurons were observed in the VP and the SI. Ottersen (1980) noted that the VP projects to the LA and the BLA while the SI does not project to the LA. Groenewegen et al. (1993) reported VP projections mainly to the BLA but less to the LA, BMA, and the CeA. A similar pattern was observed with the case RETT9 in this study. Injection in RETT9 was confined to the LA. Fewer retrogradely labeled neurons were observed in the SI, SI/EA, and the VP in RETT9 compared to RETT1 and RETT7. A recent study by Agostinelli et al. (2019) also confirms this finding. Following anterograde tracing from basal forebrain nuclei, they concluded that basal forebrain projections from the SI and the hDB/MCPO do not reach the LA but the BLA. Similarly, in RETT9, only a few retrogradely labeled neurons were encountered in the hDB/MCPO. Agostinelli et al. (2019) reported the highest number of BLA-projecting neurons in the SI. In addition, these neurons were preferentially located in the sublenticular SI or the EA. This thesis consistently revealed the highest percentage of BLA-projecting neurons in the SI/EA. For basal forebrain projections to the CeA and the MeA, Grove (1988a) made a distinction. While dorsal SI projected to the CeA, ventral SI projected to the MeA. A similar distinction was observed between RETT11 and RETT12 in this study. RETT11 injection was confined to the MeA while RETT12 injection was confined to the CeA. Many of the retrogradely labeled SI/EA neurons in RETT11 were ventrally located as can be seen in Figure 23. In RETT12, however, dorsal part of the SI was occupied.

Grove (1988a) described projections to the lateral and medial BNST from the dorsal and ventral SI, respectively. This was also in line with the projections observed in this study. Lateral and medial BNST injections revealed distinctions in basal forebrain projections. In RETT10, BNST injection was confined to the BNST lateral division, posterior part (STLP). Retrogradely labeled neurons in the SI/EA were preferentially located in dorsal parts. More ventrally, there were not many labeled neurons in the hDB/MCPO. In RETT12, however, BNST injection was confined to BNST medial division, posteromedial part (STMPM). Many of the retrogradely labeled neurons were in the ventral SI. In addition, many labeled neurons were observed in the hDB/MCPO ventral to the SI. Agostinelli et al. (2019) described more projections to the BNST from caudal as opposed to rostral basal forebrain levels. Results of this study confirm that observation. Anteriorly, there were projections to the BNST from the hDB/MCPO but not from the VP. Posteriorly, however, number of the retrogradely labeled neurons increased, especially with those in the SI/EA. These results are also in line with the extended amygdala conceptualization. Extended amygdala consists of two corridors. One corridor passes from the CeA to the lateral BNST through the dorsolateral SI. The other corridor runs from the MeA to the medial BNST through the ventromedial SI (Alheid, 2003; Alheid & Heimer, 1988; Alheid & Heimer, 1996). CeA and lateral BNST injections revealed retrogradely labeled neurons in the dorsal SI while MeA and medial BNST injections revealed retrogradely labeled neurons in the ventral SI.

As mentioned above, Mascagni and McDonald (2009) showed that PV-immunopositive basal forebrain neurons project to the basolateral complex. They emphasized that only a small proportion (10%) of the amygdala-projecting neurons were PV-immunopositive. This is expectable considering the heterogeneity in the

cellular makeup of basal forebrain neurons. PV immunohistochemistry in this study also revealed a small number of double-labeled neurons. Only five neurons (2%) located in the VP were beads and PV double-labeled. Smaller proportion found in this study may be due to the basal forebrain nuclei observed. Majority of the double-labeled neurons Mascagni and McDonald (2009) reported were located in the fundus striati and the ventral portions of the GP (refer to Figure 3 in Mascagni and McDonald (2009)) whereas double-labeled neurons in the VP, hDB/MCPO, and the SI constituted the minority as in this study. In addition, in this study, double-labeled neurons in the GP and the fundus striati/IPAC region were not included to cell counts as they were not the nuclei of interest. Also confirming the small proportion of PV-immunopositive basal forebrain neurons projecting to the amygdala, Do et al. (2016) demonstrated that cholinergic but not the PV- or SOM-immunopositive GABAergic neurons constitute the majority of the basal forebrain projections to the amygdala. In line with the 1% of PV-immunopositive neurons projecting to the CeA and the MeA in this study, they found that both medial and striatum-like central amygdalar nuclei received 1% of PV-immunopositive basal forebrain projections (Do et al., 2016).

Immunohistochemical characterization of BNST-projecting basal forebrain neurons is scarce in the literature. Do et al. (2016) revealed less than 1% of PV-immunopositive neurons projecting to the posterior division of the BNST. This proportion was 2% for the anterior division of the BNST. In this study, in eight sections immunostained for PV, no beads-PV double-labeled neurons were encountered in the basal forebrain nuclei. As explained in the results, PV single-labeled neurons were not very numerous in the basal forebrain. Even though testing more sections could reveal double-labeled neurons, proportion would not be high as the results of this study and those by Do et al. (2016) suggest. In addition, no beads-

SATB1 double-labeled neurons were encountered in basal forebrain nuclei. SATB1-immunopositive neurons were particularly abundant in the hDB/MCPO. This observation is in line with the findings by Huang et al. (2011). They performed SATB1 immunostaining in mice and similarly reported heavy labeling in both the hDB and the vDB. SATB1-immunoreactivity in the hippocampus shows a subpopulation of PV interneurons (Unal et al., 2018; Viney et al., 2013). There is also evidence that SATB1 is crucial in the differentiation and survival of the PV and SOM cortical interneurons. Conditional removal of SATB1 also reduces the number of PV- and SOM-immunopositive interneurons (Close et al., 2012). These findings suggest that SATB1-immunopositive neurons of the basal forebrain can be GABAergic. However, whether they show PV-immunoreactivity requires future work.

In contrast to the small proportion of beads-PV and beads-SATB1 double-labeled neurons, beads-CB double-labeled neurons revealed higher proportions (see Figures 16, 21, and 27). Number of double-labeled neurons were particularly high following CeA and MeA injections. To my knowledge, no study has described CB-immunopositive basal forebrain neurons projecting to the BLA, CeA, MeA, and the BNST. However, one must be careful calling these neurons GABAergic as there is evidence showing the existence of CB-immunopositive glutamatergic neurons in the basal forebrain (McKenna et al., 2021). McKenna et al. (2021) described CB-immunopositive vesicular glutamate transporter 2 (VGluT2)-tdTomato neurons in the VP, SI, hDB, and the MCPO. Double-labeled neurons constituted approximately 20% of all VGluT2-tdTomato glutamatergic neurons. Gritti et al. (2003) carried out histochemical characterization of basal forebrain neurons for PV, CB, and CR in addition to GAD and phosphate-activated glutaminase (PAG). While >90% of PV-

immunopositive neurons were GAD-immunopositive GABAergic neurons, this proportion was <10% for CB-immunopositive group. In addition, >40% of the CB-immunopositive neurons were PAG-immunopositive glutamatergic neurons. Present study revealed highest percentage of beads-CB double-labeling in the SI/EA for CeA- and MeA- projecting neurons. Agostinelli et al. (2019) reported that the GABAergic and glutamatergic SI neurons project to the CeA. This finding similarly suggests that CB-immunopositive projection neurons can be both GABAergic and glutamatergic. Based on these findings, CB-immunopositive neurons in this study are referred to as putative GABAergic neurons.

CB-immunopositive glutamatergic neurons described by McKenna et al. (2021) were observed in anterior basal forebrain levels. They selected three sections from Bregma 0.38 mm, 0.014 mm, and −0.10 mm to represent rostral, medial, and caudal basal forebrain levels, respectively. They reported no difference along this rostrocaudal axis. However, these basal forebrain levels are too rostral compared to the levels observed in this study. Bregma −0.10 mm in the mouse brain corresponds approximately to Bregma −0.48 mm in the rat. As mentioned above, present study observed basal forebrain sections until Bregma −1.44 mm. Looking at CB immunoreactivity in glutamatergic neurons in more caudal basal forebrain levels might reveal different results. In addition, evidence suggests that cholinergic, GABAergic, and glutamatergic neurons of the basal forebrain are distinct subgroups (Agostinelli et al., 2019; Gritti et al., 2006; Gritti, Mainville, & Jones, 1993). However, there are findings pointing overlaps between these groups. Nickerson Poulin, Guerci, El Mestikawy, and Semba (2006) described a basal forebrain neuronal subpopulation double-labeled for ChAT and vesicular glutamate transporter 3 (VGluT3) projecting to the BLA. Approximately 30% of the cholinergic neurons in

the VP also contained VGluT3. Retrograde tracing of cholinergic neurons from the BLA revealed that almost 50% in the VP are also labeled for VGluT3. Future work should focus on a more detailed characterization of basal forebrain neurons. Specifically, whether CB-immunopositive neurons projecting to the amygdala and the BNST are GABAergic and/or glutamatergic should be examined.

5.1 Limitations

Current study has several weaknesses and limitations that need to be pointed out. First, green Retrobeads did not work as well as red Retrobeads. They labeled less neurons compared to red beads. In addition, green beads labeled neurons were harder to detect due to low signal. Counterbalancing red and green beads injections to the amygdala and the BNST overcame this problem to a certain degree. However, number of neurons labeled with green beads might be an underestimation of actual numbers.

Second, tracing and immunohistochemistry data for centromedial amygdala injections had to be pooled. CeA and MeA were injected in one case each which made it impossible to compare the consistency of the results within CeA and MeA injections. CeA injection was in the CeM, probably also covering some parts of the CeL but not the CeC. MeA injection was in the MePD, probably also covering some parts of CeM. Earlier tracing studies described basal forebrain projections to the CeA and the MeA (Grove, 1988a; Ottersen, 1980). For instance, following HRP injections to the MeA, Ottersen (1980) showed that the MeA received projections from the SI. However, these projections were observed in rostral MeA injections compared to caudal MeA injections. Following CeA injections, HRP-labeled neurons were again

observed in the SI. However, while a dorsal CeA injection labeled many neurons in the SI, a more ventral CeA injection in approximately the same levels labeled a modest number of neurons in the SI. Generally, tracing results in this study are in line with those prior reports. However, topographical differences in basal forebrain projections with PV- and CB-immunopositive subgroups to different parts of the CeA and the MeA could not be described.

Third, both the amygdala and the BNST are sexually dimorphic structures. MeA shows greater volume in male than in female rats (Mizukami, Nishizuka, & Arai, 1983) and its synaptic organization differs between sexes (Cooke & Woolley, 2005; Nishizuka & Arai, 1981; Nishizuka & Arai, 1983). MeA activity also shows sexual dimorphism. MeA units in mice become more responsive to opposite sex stimuli compared to same sex stimuli (Bergan, Ben-Shaul, & Dulac, 2014) and MeA GABAergic neurons are associated with parenting behavior in females while the same neuronal group is involved in both parenting behavior and infanticide in males (Chen et al., 2019). Similarly, BNST nuclei show sexual dimorphism in both humans and rats. As the central subdivision of the BNST is larger and contains more neurons in men than in women (Swaab, 2007), the encapsulated nucleus of the BNST is larger and contains more neurons in male rats than in female rats (Hines, Allen, & Gorski, 1992; Simerly, 1990). More CRF is expressed in the dorsolateral BNST in female mice compared to male mice (Uchida et al., 2019) and predator odor exposure causes more CRF mRNA expression in the BNST of male compared to female GAD67 mice (Janitzky et al., 2014). Vasopressin-expressing neurons are also more numerous in the BNST of male rats compared to female rats (Miller, Vician, Clifton, & Dorsa, 1989). Considering these differences, it is also possible to expect

differences between sexes in basal forebrain GABAergic projections to the amygdala and the BNST. Therefore, female rats would be a valuable addition to this study.

5.2 Future directions

Findings of this study present an important step towards describing the basal forebrain GABAergic projections to the amygdala and the BNST, two structures underlying fear and anxiety, respectively. Subsequent studies in our laboratory will integrate these findings with chemogenetics and optogenetics to selectively activate and inactivate projecting GABAergic subpopulations. These studies, coupled with behavioral phasic and sustained fear paradigms, will prove valuable in characterizing neuronal groups and networks leading to fear and anxiety. For instance, CB-immunopositive neurons in the VP and the SI/EA will be selectively inactivated while animals are introduced to fear and anxiety tasks and the impact of silencing this neuronal subpopulation will be observed through animals' behavior.

According to my hypotheses explained in chapter two, basal forebrain GABAergic projections to the amygdala and the BNST contribute to fear and anxiety learning and memory processes through their contribution to oscillatory activities in these structures. Present study and the subsequent selective activation/inactivation studies, however, do not directly examine the contribution of basal forebrain GABAergic projections to the oscillations in the amygdala and the BNST. A collaboration study in progress will directly test this contribution to theta oscillations in the amygdala. In this study, a 1000-cell biophysical BLA model with its local circuitry and external input is created based on the model by Hummos and Nair (2017). Local circuitry includes principal neurons as well as PV-, CB-, and calretinin

(CR)-immunopositive interneurons. External input includes excitatory cortical/thalamic input as well as basal forebrain cholinergic and GABAergic input. Information used in this study including single cell anatomical information, parameter values, and synaptic properties were taken from our observations and the literature. It is hypothesized that local theta oscillations emerge when both the non-rhythmic cholinergic input and the rhythmic GABAergic input of the basal forebrain are present in addition to the constant excitatory thalamic/cortical input, as is the case for the hippocampus (Smythe, Colom, & Bland, 1992). Following the case in the hippocampus (Yoder & Pang, 2005), removing the cholinergic or the GABAergic basal forebrain input alone decreases the theta power in the BLA. In addition, the BLA theta oscillation ceases completely when the rhythmic GABAergic input is cut together either the cholinergic input or the similarly non-rhythmic thalamic/cortical input. So far, the model has produced local field potentials in the theta range. Next step will be to test our hypotheses by selectively cutting certain inputs to the BLA. Findings of this modeling study will be complementary to the present study in improving our understanding of circuitries underlying fear and anxiety.

Characterization of specific neuronal circuits underlying fear and anxiety will not only improve but also alter our current understanding of a variety of psychopathologies including depressive, anxiety, and trauma- and stressor-related disorders. Cell type-specific drugs selectively targeting only some of the neuronal populations or circuits will be produced to substantially increase treatment effectiveness with less side effects. Therefore, the ultimate goal of these studies will be to discover neuronal groups and networks that have a therapeutic potential.

APPENDIX A

ETHICS COMMITTEE APPROVAL

T.C.
BOĞAZİÇİ ÜNİVERSİTESİ
Kurumsal Hayvan Deneyleri Yerel Etik Kurulu (Bühadyek)

Sayı : 44697215-050.01.04-E.7371 29/04/2020
Konu : 2020-10 Kodlu Başvurunuz
Hakkında

Sayın Dr. Öğr. Üyesi Güneş ÜNAL
Psikoloji Bölüm Başkanlığı - Öğretim Üyesi

Yürütücülüğünü üstlendiğiniz " Wistar sıçanlarında amigdala ve BNST'ye bazal önbeyin GABAerjik projeksiyonları: Retrograd boyama çalışması (Basal forebrain GABAergic projections to the amygdala and the BNST in Wistar rats: A retrograde tract-tracing study" adlı, 25.02.2020 başvuru tarihli ve 2020-10 kodlu başvurunuz, Boğaziçi Üniversitesi Kurumsal Hayvan Deneyleri Yerel Etik Kurulu'nun (BÜHADYEK) 20.02.2020 tarihli toplantısında görüşülmüş ve KABUL edilmiştir..

Bu karar tüm üyelerin toplantıya on-line olarak katılımıyla ve oybirliği ile alınmıştır. COVID-19 önlemleri nedeniyle üyelerden ıslak imza alınamadığından bu onam mektubu tüm üyeler adına Komisyon Başkanı tarafından e-imzalanmıştır

Saygılarımızla bilginize sunarız

e-imzalıdır
Prof. Dr. Burak GÜÇLÜ
Komisyon Başkanı

Adres:34342 Bebek-İstanbul
Telefon:0212 287 17 53 Faks:0212 265 70 06
Elektronik Ağ:www.boun.edu.tr
Bilgi için: Lale DİLEK

Bu belge 5070 sayılı Elektronik İmza Kanununun 5. Maddesi gereğince güvenli elektronik imza ile imzalanmıştır.

APPENDIX B

STEREOTAXIC SURGERY LOG SHEET

BEHAVIORAL NEUROSCIENCE LABORATORY SURGERY LOG SHEET						
Species/Sex	Rat	F/M	Strain	Wistar	Animal ID	
Pre-op weight (g)			Operation date		Operator	
					Birthdate	
Surgery goal						
Stereotaxic targets:						
From Bregma AP: From Bregma ML: From Dura DV:						
Bregma Point:						
Calculated AP: Calculated ML: Calculated DV:						
Anesthesia						
DRUG	DOSE		ROUTE	TIME		EFFECT / NOTES

APPENDIX C

POST-OPERATIVE ASSESSMENT CHECKLIST

DAVRANIŞSAL SİNİRBİLİM LABORATUVARI								
OPERASYON/AMELİYAT SONRASI HAYVAN SAĞLIĞI TAKİP ÇİZELGESİ (POST-OPERATIVE ASSESSMENT CHECKLIST)								
Tür / Cinsiyet		F / M	Suş			Denek #		
Pre-op ağırlık (g)			Tarih			Cerrah		
	Op. /Ameliyat günü	Operasyon sonrası						
					Ölçütler 3 gün sonunda normal değerler dışında ise doldurulacak.			
		1. gün	2. gün	3. gün	4. gün	5. gün	6. gün	7. gün
Değerlendiren								
Değerlendirme saati								
Ağırlık (g)								
Normal belirti ve davranışlara 0 veriniz, anormal durumları 1 (hafif), 2 (orta) veya 3 (ciddi) olarak kaydediniz.								
GENEL KLİNİK BELİRTİLER								
İnaktivite								
Kambur duruş								
Tüy dökülmesi								
Tüyde renk değişimi								
Göz kanlanması								
Burun akıntısı								
OPERASYON BÖLGESİ DEĞERLENDİRMESİ								
İltihaplanma								
Dikiş çıkması								
Kanama								
DAVRANIŞSAL AĞRI BELİRTİLERİ (HAYVANI EN AZ 5 DAKİKA BOYUNCA GÖZLEMLEYİNİZ)								
Yana kıvrılma/düşme								
Kambur çıkarma								
Sendeleme								
Uzuv seğirmesi								

SU TÜKETİMİ (GÜNLÜK ORTALAMA SU TÜKETİMİ SIÇANLARDA VÜCUT AĞIRLIĞININ %10'U, FARELERDE %15'İ KADAR OLMALIDIR)								
Dolu şişe ağırlığı								
Şişenin mevcut ağırlığı								
Ağırlık farkı (g ≈ ml)								
POST-OP MÜDAHALE (GEREKLİ İSE)								
İlaç								
Doz								
Sonlandırma								
NOTLAR								

REFERENCES

Agostinelli, L. J., Geerling, J. C., & Scammell, T. E. (2019). Basal forebrain subcortical projections. *Brain Structure and Function*, *224*(3), 1097–1117. https://doi.org/10.1007/s00429-018-01820-6

Alheid, G. F. (2003). Extended amygdala and basal forebrain. *Annals of the New York Academy of Sciences*, *985*(1), 185–205. https://doi.org/10.1111/j.1749-6632.2003.tb07082.x

Alheid, G. F., & Heimer, L. (1988). New perspectives in basal forebrain organization of special relevance for neuropsychiatric disorders: The striatopallidal, amygdaloid, and corticopetal components of substantia innominata. *Neuroscience*, *27*(1), 1–39. https://doi.org/10.1016/0306-4522(88)90217-5

Alheid, G. F., & Heimer, L. (1996). Chapter 28 Theories of basal forebrain organization and the "emotional motor system." In G. Holstege, R. Bandler, & C. B. Saper (Eds.), *The Emotional Motor System* (Vol. 107, pp. 461–484). Progress in Brain Research. https://doi.org/10.1016/S0079-6123(08)61882-8

American Psychiatric Association. (2013). *Diagnostic and statistical manual of mental disorders* (5th ed.). Washington, DC: American Psychiatric Publishing.

Apps, R., & Ruigrok, T. J. H. (2007). A fluorescence-based double retrograde tracer strategy for charting central neuronal connections. *Nature Protocols*, *2*(8), 1862–1868. https://doi.org/10.1038/nprot.2007.263

Armbruster, B. N., Li, X., Pausch, M. H., Herlitze, S., & Roth, B. L. (2007). Evolving the lock to fit the key to create a family of G protein-coupled receptors potently activated by an inert ligand. *Proceedings of the National Academy of Sciences*, *104*(12), 5163–5168. https://doi.org/10.1073/pnas.0700293104

Baisden, R. H., Woodruff, M. L., & Hoover, D. B. (1984). Cholinergic and non-cholinergic septo-hippocampal projections: A double-label horseradish peroxidase-acetylcholinesterase study in the rabbit. *Brain Research*, *290*(1), 146–151. https://doi.org/10.1016/0006-8993(84)90745-5

Bergan, J. F., Ben-Shaul, Y., & Dulac, C. (2014). Sex-specific processing of social cues in the medial amygdala. *ELife*, *3*, e02743. https://doi.org/10.7554/eLife.02743

Brauer, K., Schober, A., Wolff, J. R., Winkelmann, E., Luppa, H., Lüth, H. J., & Böttcher, H. (1991). Morphology of neurons in the rat basal forebrain nuclei: Comparison between NADPH-diaphorase histochemistry and immunohistochemistry of glutamic acid decarboxylase, choline acetyltransferase, somatostatin and parvalbumin. *Journal Fur Hirnforschung*, *32*(1), 1–17. Retrieved from http://europepmc.org/abstract/MED/1687412

Brown, J. S., Kalish, H. I., & Farber, I. E. (1951). Conditioned fear as revealed by magnitude of startle response to an auditory stimulus. *Journal of Experimental Psychology*, *41*, 317–328. https://doi.org/10.1037/h0060166

Buzsaki, G., Bickford, R. G., Ponomareff, G., Thal, L. J., Mandel, R., & Gage, F. H. (1988). Nucleus basalis and thalamic control of neocortical activity in the freely moving rat. *The Journal of Neuroscience*, *8*(11), 4007–4026. https://doi.org/10.1523/JNEUROSCI.08-11-04007.1988

Cape, E. G., Manns, I. D., Alonso, A., Beaudet, A., & Jones, B. E. (2000). Neurotensin-induced bursting of cholinergic basal forebrain neurons promotes γ and θ cortical activity together with waking and paradoxical Sleep. *The Journal of Neuroscience*, *20*(22), 8452–8461. https://doi.org/10.1523/JNEUROSCI.20-22-08452.2000

Carlsen, J., Záborszky, L., & Heimer, L. (1985). Cholinergic projections from the basal forebrain to the basolateral amygdaloid complex: A combined retrograde fluorescent and immunohistochemical study. *Journal of Comparative Neurology*, *234*(2), 155–167. https://doi.org/10.1002/cne.902340203

Casada, J. H., & Dafny, N. (1991). Restraint and stimulation of bed nucleus of the stria terminalis produce similar stress-like behaviors. *Brain Research Bulletin*, *27*(2), 207–212. https://doi.org/10.1016/0361-9230(91)90069-V

Chen, P. B., Hu, R. K., Wu, Y. E., Pan, L., Huang, S., Micevych, P. E., & Hong, W. (2019). Sexually dimorphic control of parenting behavior by the medial amygdala. *Cell*, *176*(5), 1206-1221.e18. https://doi.org/10.1016/j.cell.2019.01.024

Close, J., Xu, H., De Marco García, N., Batista-Brito, R., Rossignol, E., Rudy, B., & Fishell, G. (2012). Satb1 is an activity-modulated transcription factor required for the terminal differentiation and connectivity of medial ganglionic eminence-derived cortical interneurons. *The Journal of Neuroscience*, *32*(49), 17690–17705. https://doi.org/10.1523/JNEUROSCI.3583-12.2012

Cooke, B. M., & Woolley, C. S. (2005). Sexually dimorphic synaptic organization of the medial amygdala. *The Journal of Neuroscience*, *25*(46), 10759–10767. https://doi.org/10.1523/JNEUROSCI.2919-05.2005

Coons, A. H. (1958). Fluorescent antibody methods. *General Cytochemical Methods*, *1*, 399–422.

Davis, M., Walker, D. L., Miles, L., & Grillon, C. (2010). Phasic vs sustained fear in rats and humans: Role of the extended amygdala in fear vs anxiety. *Neuropsychopharmacology*, *35*(1), 105–135. https://doi.org/10.1038/npp.2009.109

Day, H. E. W., Curran, E. J., Watson Jr., S. J., & Akil, H. (1999). Distinct neurochemical populations in the rat central nucleus of the amygdala and bed nucleus of the stria terminalis: Evidence for their selective activation by interleukin-1β. *Journal of Comparative Neurology*, *413*(1), 113–128. https://doi.org/10.1002/(SICI)1096-9861(19991011)413:1<113::AID-CNE8>3.0.CO;2-B

de Olmos, J. S. (1972). The amygdaloid projection field in the rat as studied with the cupric-silver method. In *The neurobiology of the amygdala* (pp. 145–204). Springer.

Deisseroth, K. (2011). Optogenetics. *Nature Methods*, *8*(1), 26–29. https://doi.org/10.1038/nmeth.f.324

Dinopoulos, A., Parnavelas, J. G., Uylings, H. B. M., & van Eden, C. G. (1988). Morphology of neurons in the basal forebrain nuclei of the rat: A Golgi study. *Journal of Comparative Neurology*, *272*(4), 461–474. https://doi.org/10.1002/cne.902720402

Do, J. P., Xu, M., Lee, S.-H., Chang, W.-C., Zhang, S., Chung, S., … Dan, Y. (2016). Cell type-specific long-range connections of basal forebrain circuit. *Elife*, *5*, e13214. https://doi.org/ 10.7554/eLife.13214

Dong, H.-W., Petrovich, G. D., & Swanson, L. W. (2001). Topography of projections from amygdala to bed nuclei of the stria terminalis. *Brain Research Reviews*, *38*(1), 192–246. https://doi.org/10.1016/S0165-0173(01)00079-0

Dong, H.-W., Petrovich, G. D., Watts, A. G., & Swanson, L. W. (2001). Basic organization of projections from the oval and fusiform nuclei of the bed nuclei of the stria terminalis in adult rat brain. *Journal of Comparative Neurology*, *436*(4), 430–455. https://doi.org/10.1002/cne.1079

Durkin, T. (1989). Central cholinergic pathways and learning and memory processes: Presynaptic aspects. *Comparative Biochemistry and Physiology Part A: Physiology*, *93*(1), 273–280. https://doi.org/10.1016/0300-9629(89)90216-8

Eichenbaum, H. (2017). Prefrontal–hippocampal interactions in episodic memory. *Nature Reviews Neuroscience*, *18*(9), 547–558. https://doi.org/10.1038/nrn.2017.74

Ekman, P. (1992). An argument for basic emotions. *Cognition and Emotion*, *6*(3–4), 169–200. https://doi.org/10.1080/02699939208411068

Everitt, B. J., & Robbins, T. W. (1997). Central cholinergic systems and cognition. *Annual Review of Psychology*, *48*(1), 649–684. https://doi.org/10.1146/annurev.psych.48.1.649

Fendt, M., Endres, T., & Apfelbach, R. (2003). Temporary inactivation of the bed nucleus of the stria terminalis but not of the amygdala blocks freezing induced by trimethylthiazoline, a component of fox feces. *The Journal of Neuroscience*, *23*(1), 23–28. https://doi.org/10.1523/JNEUROSCI.23-01-00023.2003

File, S. E., & Hyde, J. R. G. (1978). Can social interaction be used to measure anxiety? *British Journal of Pharmacology*, *62*(1), 19–24. https://doi.org/10.1111/j.1476-5381.1978.tb07001.x

Freund, T. F., & Buzsáki, G. (1996). Interneurons of the hippocampus. *Hippocampus*, *6*(4), 347–470. https://doi.org/10.1002/(SICI)1098-1063(1996)6:4<347::AID-HIPO1>3.0.CO;2-I

Freund, T. F. (1989). GABAergic septohippocampal neurons contain parvalbumin. *Brain Research*, *478*(2), 375–381. https://doi.org/10.1016/0006-8993(89)91520-5

Freund, T. F., & Antal, M. (1988). GABA-containing neurons in the septum control inhibitory interneurons in the hippocampus. *Nature*, *336*(6195), 170–173. https://doi.org/10.1038/336170a0

Frotscher, M., & Léránth, C. (1985). Cholinergic innervation of the rat hippocampus as revealed by choline acetyltransferase immunocytochemistry: A combined light and electron microscopic study. *Journal of Comparative Neurology*, *239*(2), 237–246. https://doi.org/10.1002/cne.902390210

Gangadharan, G., Shin, J., Kim, S.-W., Kim, A., Paydar, A., Kim, D.-S., … Shin, H.-S. (2016). Medial septal GABAergic projection neurons promote object exploration behavior and type 2 theta rhythm. *Proceedings of the National Academy of Sciences*, *113*(23), 6550–6555. https://doi.org/10.1073/pnas.1605019113

Gärtner, U., Härtig, W., Riedel, A., Brauer, K., & Arendt, T. (2002). Immunocytochemical evidence for the striatal nature of the rat lateral part of interstitial nucleus of the posterior limb of the anterior commissure (IPAC). *Journal of Chemical Neuroanatomy*, *24*(2), 117–125. https://doi.org/10.1016/s0891-0618(02)00035-2

Gerashchenko, D., Salin-Pascual, R., & Shiromani, P. J. (2001). Effects of hypocretin–saporin injections into the medial septum on sleep and hippocampal theta. *Brain Research*, *913*(1), 106–115. https://doi.org/10.1016/S0006-8993(01)02792-5

Gray, T. S., & Magnuson, D. J. (1987). Neuropeptide neuronal efferents from the bed nucleus of the stria terminalis and central amygdaloid nucleus to the dorsal vagal complex in the rat. *Journal of Comparative Neurology*, *262*(3), 365–374. https://doi.org/10.1002/cne.902620304

Gritti, I., Henny, P., Galloni, F., Mainville, L., Mariotti, M., & Jones, B. E. (2006). Stereological estimates of the basal forebrain cell population in the rat, including neurons containing choline acetyltransferase, glutamic acid decarboxylase or phosphate-activated glutaminase and colocalizing vesicular glutamate transporters. *Neuroscience*, *143*(4), 1051–1064. https://doi.org/10.1016/j.neuroscience.2006.09.024

Gritti, I., Mainville, L., & Jones, B. E. (1993). Codistribution of GABA- with acetylcholine-synthesizing neurons in the basal forebrain of the rat. *Journal of Comparative Neurology*, *329*(4), 438–457. https://doi.org/10.1002/cne.903290403

Gritti, I., Manns, I. D., Mainville, L., & Jones, B. E. (2003). Parvalbumin, calbindin, or calretinin in cortically projecting and GABAergic, cholinergic, or glutamatergic basal forebrain neurons of the rat. *Journal of Comparative Neurology*, *458*(1), 11–31. https://doi.org/10.1002/cne.10505

Groenewegen, H. J., Berendse, H. W., & Haber, S. N. (1993). Organization of the output of the ventral striatopallidal system in the rat: Ventral pallidal efferents. *Neuroscience*, *57*(1), 113–142. https://doi.org/10.1016/0306-4522(93)90115-V

Grove, E. A. (1988a). Efferent connections of the substantia innominata in the rat. *Journal of Comparative Neurology*, *277*(3), 347–364. https://doi.org/10.1002/cne.902770303

Grove, E. A. (1988b). Neural associations of the substantia innominata in the rat: Afferent connections. *Journal of Comparative Neurology*, *277*(3), 315–346. https://doi.org/10.1002/cne.902770302

Gungor, N. Z., & Paré, D. (2016). Functional heterogeneity in the bed nucleus of the stria terminalis. *The Journal of Neuroscience*, *36*(31), 8038–8049. https://doi.org/10.1523/JNEUROSCI.0856-16.2016

Haber, S. N., Groenewegen, H. J., Grove, E. A., & Nauta, W. J. H. (1985). Efferent connections of the ventral pallidum: Evidence of a dual striato pallidofugal pathway. *Journal of Comparative Neurology*, *235*(3), 322–335. https://doi.org/10.1002/cne.902350304

Hangya, B., Borhegyi, Z., Szilágyi, N., Freund, T. F., & Varga, V. (2009). GABAergic neurons of the medial septum lead the hippocampal network during theta activity. *The Journal of Neuroscience*, *29*(25), 8094–8102. https://doi.org/10.1523/JNEUROSCI.5665-08.2009

Hassani, O. K., Lee, M. G., Henny, P., & Jones, B. E. (2009). Discharge profiles of identified GABAergic in comparison to cholinergic and putative glutamatergic basal forebrain neurons across the sleep–wake cycle. *The Journal of Neuroscience*, *29*(38), 11828–11840. https://doi.org/10.1523/JNEUROSCI.1259-09.2009

Hasselmo, M. E. (2006). The role of acetylcholine in learning and memory. *Current Opinion in Neurobiology*, *16*(6), 710–715. https://doi.org/10.1016/j.conb.2006.09.002

Henke, P. G. (1984). The bed nucleus of the stria terminalis and immobilization-stress: Unit activity, escape behaviour, and gastric pathology in rats. *Behavioural Brain Research*, *11*(1), 35–45. https://doi.org/10.1016/0166-4328(84)90006-8

Hewitt, S. M., Baskin, D. G., Frevert, C. W., Stahl, W. L., & Rosa-Molinar, E. (2014). Controls for immunohistochemistry: The histochemical society's standards of practice for validation of immunohistochemical assays. *Journal of Histochemistry & Cytochemistry*, *62*(10), 693–697. https://doi.org/10.1369/0022155414545224

Hines, M., Allen, L. S., & Gorski, R. A. (1992). Sex differences in subregions of the medial nucleus of the amygdala and the bed nucleus of the stria terminalis of the rat. *Brain Research*, *579*(2), 321–326. https://doi.org/10.1016/0006-8993(92)90068-K

Hitchcock, J., & Davis, M. (1986). Lesions of the amygdala, but not of the cerebellum or red nucleus, block conditioned fear as measured with the potentiated startle paradigm. *Behavioral Neuroscience*, *100*(1), 11–22. https://doi.org/10.1037//0735-7044.100.1.11

Hitchcock, J. M., & Davis, M. (1991). Efferent pathway of the amygdala involved in conditioned fear as measured with the fear-potentiated startle paradigm. *Behavioral Neuroscience*, *105*(6), 826–842. https://doi.org/10.1037//0735-7044.105.6.826

Huang, Y., Zhang, L., Song, N.-N., Hu, Z.-L., Chen, J.-Y., & Ding, Y.-Q. (2011). Distribution of Satb1 in the central nervous system of adult mice. *Neuroscience Research*, *71*(1), 12–21. https://doi.org/10.1016/j.neures.2011.05.015

Hummos, A., & Nair, S. S. (2017). An integrative model of the intrinsic hippocampal theta rhythm. *PLOS ONE*, *12*(8), e0182648. https://doi.org/10.1371/journal.pone.0182648

Janitzky, K., Peine, A., Kröber, A., Yanagawa, Y., Schwegler, H., & Roskoden, T. (2014). Increased CRF mRNA expression in the sexually dimorphic BNST of male but not female GAD67 mice and TMT predator odor stress effects upon spatial memory retrieval. *Behavioural Brain Research*, *272*, 141–149. https://doi.org/10.1016/j.bbr.2014.06.020

Johnston, J. B. (1923). Further contributions to the study of the evolution of the forebrain. *Journal of Comparative Neurology*, *35*(5), 337–481. https://doi.org/10.1002/cne.900350502

Ju, G., & Swanson, L. W. (1989). Studies on the cellular architecture of the bed nuclei of the stria terminalis in the rat: I. Cytoarchitecture. *Journal of Comparative Neurology*, *280*(4), 587–602. https://doi.org/10.1002/cne.902800409

Kádár, A., Wittmann, G., Liposits, Z., & Fekete, C. (2009). Improved method for combination of immunocytochemistry and Nissl staining. *Journal of Neuroscience Methods*, *184*(1), 115–118. https://doi.org/10.1016/j.jneumeth.2009.07.010

Katz, L. C., Burkhalter, A., & Dreyer, W. J. (1984). Fluorescent latex microspheres as a retrograde neuronal marker for in vivo and in vitro studies of visual cortex. *Nature*, *310*(5977), 498–500. https://doi.org/10.1038/310498a0

Katz, L. C., & Iarovici, D. M. (1990). Green fluorescent latex microspheres: A new retrograde tracer. *Neuroscience*, *34*(2), 511–520. https://doi.org/10.1016/0306-4522(90)90159-2

Kennedy, S. H. (2006). A review of antidepressant treatments today. *European Neuropsychopharmacology*, *16*, S619–S623. https://doi.org/10.1016/S0924-977X(06)70007-4

Klausberger, T., & Somogyi, P. (2008). Neuronal diversity and temporal dynamics: The unity of hippocampal circuit operations. *Science*, *321*(5885), 53–57. https://doi.org/10.1126/science.1149381

Köhler, C., Chan-Palay, V., & Wu, J.-Y. (1984). Septal neurons containing glutamic acid decarboxylase immunoreactivity project to the hippocampal region in the rat brain. *Anatomy and Embryology*, *169*(1), 41–44. https://doi.org/10.1007/BF00300585

Krettek, J. E., & Price, J. L. (1978). Amygdaloid projections to subcortical structures within the basal forebrain and brainstem in the rat and cat. *Journal of Comparative Neurology*, *178*(2), 225–253. https://doi.org/10.1002/cne.901780204

LeDoux, J. E., Iwata, J., Cicchetti, P., & Reis, D. J. (1988). Different projections of the central amygdaloid nucleus mediate autonomic and behavioral correlates of conditioned fear. *The Journal of Neuroscience*, *8*(7), 2517–2529. https://doi.org/10.1523/JNEUROSCI.08-07-02517.1988

Lee, M. G., Chrobak, J. J., Sik, A., Wiley, R. G., & Buzsáki, G. (1994). Hippocampal theta activity following selective lesion of the septal cholinergic system. *Neuroscience*, *62*(4), 1033–1047. https://doi.org/10.1016/0306-4522(94)90341-7

Lewis, P. R., & Shute, C. C. D. (1967). The cholinergic limbic system: Projections to hippocampal formation, medial cortex, nuclei of the ascending cholinergic reticular system, and the subfornical organ and supra-optic crest. *Brain*, *90*(3), 521–540. https://doi.org/ 10.1093/brain/90.3.521

MacLean, P. D. (1949). Psychosomatic disease and the “visceral brain”: Recent developments bearing on the Papez theory of emotion. *Psychosomatic Medicine*, *11*(6), 338–353. https://doi.org/10.1097/00006842-194911000-00003

Mascagni, F., & McDonald, A. J. (2009). Parvalbumin-immunoreactive neurons and GABAergic neurons of the basal forebrain project to the rat basolateral amygdala. *Neuroscience*, *160*(4), 805–812. https://doi.org/10.1016/j.neuroscience.2009.02.077

McDonald, A., Mascagni, F., & Zaric, V. (2012). Subpopulations of somatostatin-immunoreactive non-pyramidal neurons in the amygdala and adjacent external capsule project to the basal forebrain: Evidence for the existence of GABAergic projection neurons in the cortical nuclei and basolateral nuclear complex. *Frontiers in Neural Circuits*, *6*, 46. https://doi.org/10.3389/fncir.2012.00046

McDonald, A. J., Muller, J. F., & Mascagni, F. (2011). Postsynaptic targets of GABAergic basal forebrain projections to the basolateral amygdala. *Neuroscience*, *183*, 144–159. https://doi.org/10.1016/j.neuroscience.2011.03.027

McDonald, A. J. (2020). Chapter 1 - Functional neuroanatomy of the basolateral amygdala: Neurons, neurotransmitters, and circuits. In J. H. Urban & J. A. Rosenkranz (Eds.), *Handbook of amygdala structure and function* (Vol. 26, pp. 1–38). https://doi.org/10.1016/B978-0-12-815134-1.00001-5

McDonald, A. J., & Mascagni, F. (2002). Immunohistochemical characterization of somatostatin containing interneurons in the rat basolateral amygdala. *Brain Research*, *943*(2), 237–244. https://doi.org/10.1016/S0006-8993(02)02650-1

McKenna, J. T., Yang, C., Bellio, T., Anderson-Chernishof, M. B., Gamble, M. C., Hulverson, A., … Brown, R. E. (2021). Characterization of basal forebrain glutamate neurons suggests a role in control of arousal and avoidance behavior. *Brain Structure and Function*. https://doi.org/10.1007/s00429-021-02288-7

McNaughton, N., Ruan, M., & Woodnorth, M.-A. (2006). Restoring theta-like rhythmicity in rats restores initial learning in the Morris water maze. *Hippocampus*, *16*(12), 1102–1110. https://doi.org/10.1002/hipo.20235

Mesulam, M.-M., Mufson, E. J., Wainer, B. H., & Levey, A. I. (1983). Central cholinergic pathways in the rat: An overview based on an alternative nomenclature (Ch1–Ch6). *Neuroscience*, *10*(4), 1185–1201. https://doi.org/10.1016/0306-4522(83)90108-2

Mesulam, M. (2004). The cholinergic lesion of Alzheimer's disease: Pivotal factor or side show? *Learning & Memory* , *11*(1), 43–49. https://doi.org/10.1101/lm.69204

Miller, M. A., Vician, L., Clifton, D. K., & Dorsa, D. M. (1989). Sex differences in vasopressin neurons in the bed nucleus of the stria terminalis by in situ hybridization. *Peptides*, *10*(3), 615–619. https://doi.org/10.1016/0196-9781(89)90152-6

Mizukami, S., Nishizuka, M., & Arai, Y. (1983). Sexual difference in nuclear volume and its ontogeny in the rat amygdala. *Experimental Neurology*, *79*(2), 569–575. https://doi.org/10.1016/0014-4886(83)90235-2

Mizumori, S. J. Y., Perez, G. M., Alvarado, M. C., Barnes, C. A., & McNaughton, B. L. (1990). Reversible inactivation of the medial septum differentially affects two forms of learning in rats. *Brain Research*, *528*(1), 12–20. https://doi.org/10.1016/0006-8993(90)90188-H

Moga, M. M., Saper, C. B., & Gray, T. S. (1989). Bed nucleus of the stria terminalis: Cytoarchitecture, immunohistochemistry, and projection to the parabrachial nucleus in the rat. *Journal of Comparative Neurology*, *283*(3), 315–332. https://doi.org/10.1002/cne.902830302

Morris, R. G. M. (1981). Spatial localization does not require the presence of local cues. *Learning and Motivation*, *12*(2), 239–260. https://doi.org/10.1016/0023-9690(81)90020-5

Muller, J. F., Mascagni, F., & McDonald, A. J. (2011). Cholinergic innervation of pyramidal cells and parvalbumin-immunoreactive interneurons in the rat basolateral amygdala. *The Journal of Comparative Neurology*, *519*(4), 790–805. https://doi.org/10.1002/cne.22550

Nickerson Poulin, A., Guerci, A., El Mestikawy, S., & Semba, K. (2006). Vesicular glutamate transporter 3 immunoreactivity is present in cholinergic basal forebrain neurons projecting to the basolateral amygdala in rat. *Journal of Comparative Neurology*, *498*(5), 690–711. https://doi.org/10.1002/cne.21081

Nishizuka, M., & Arai, Y. (1983). Regional difference in sexually dimorphic synaptic organization of the medial amygdala. *Experimental Brain Research*, *49*(3), 462–465. https://doi.org/10.1007/BF00238788

Nishizuka, M., & Arai, Y. (1981). Sexual dimorphism in synaptic organization in the amygdala and its dependence on neonatal hormone environment. *Brain Research*, *212*(1), 31–38. https://doi.org/10.1016/0006-8993(81)90029-9

Nissl, F. (1894). Ueber eine neue untersuchungsmethode des centralorgans zur feststellung der localisation der nervenzellen. *Neurologisches Centralblatt*, *13*, 507-508.

O'Keefe, J., & Recce, M. L. (1993). Phase relationship between hippocampal place units and the EEG theta rhythm. *Hippocampus*, *3*(3), 317–330. https://doi.org/10.1002/hipo.450030307

Ottersen, O. P. (1980). Afferent connections to the amygdaloid complex of the rat and cat: II. Afferents from the hypothalamus and the basal telencephalon. *Journal of Comparative Neurology*, *194*(1), 267–289. https://doi.org/10.1002/cne.901940113

Pascual, M., Pérez-Sust, P., & Soriano, E. (2004). The GABAergic septohippocampal pathway in control and reeler mice: Target specificity and termination onto reelin-expressing interneurons. *Molecular and Cellular Neuroscience*, *25*(4), 679–691. https://doi.org/10.1016/j.mcn.2003.12.009

Paxinos, G., & Franklin, K. B. J. (2001). *The mouse brain in stereotaxic coordinates* (2nd edition). Academic Press.

Paxinos, G., & Watson, C. (2007). *The rat brain in stereotaxic coordinates* (6th edition). Academic Press.

Pezuk, P., Aydin, E., Aksoy, A., & Canbeyli, R. (2008). Effects of BNST lesions in female rats on forced swimming and navigational learning. *Brain Research*, *1228*, 199–207. https://doi.org/10.1016/j.brainres.2008.06.071

Pezük, P., Göz, D., Aksoy, A., & Canbeyli, R. (2006). BNST lesions aggravate behavioral despair but do not impair navigational learning in rats. *Brain Research Bulletin*, *69*(4), 416–421. https://doi.org/10.1016/j.brainresbull.2006.02.008

Pilati, N., Barker, M., Panteleimonitis, S., Donga, R., & Hamann, M. (2008). A rapid method combining Golgi and Nissl staining to study neuronal morphology and cytoarchitecture. *Journal of Histochemistry & Cytochemistry*, *56*(6), 539–550. https://doi.org/10.1369/jhc.2008.950246

Pitkänen, A., Savander, V., & LeDoux, J. E. (1997). Organization of intra-amygdaloid circuitries in the rat: An emerging framework for understanding functions of the amygdala. *Trends in Neurosciences*, *20*(11), 517–523. https://doi.org/ 10.1016/s0166-2236(97)01125-9

Richardson, R. T., & DeLong, M. R. (1988). A reappraisal of the functions of the nucleus basalis of Meynert. *Trends in Neurosciences*, *11*(6), 264–267. https://doi.org/10.1016/0166-2236(88)90107-5

Richardson, R. T., & DeLong, M. R. (1991). Functional implications of tonic and phasic activity changes in nucleus basalis neurons. R. T. Richardson (Ed.), *Activation to acquisition: Functional aspects of the basal forebrain cholinergic system* (pp. 135–166). Birkhäuser, Boston, MA. https://doi.org/10.1007/978-1-4684-0556-9_6

Richter, C. P. (1922). A behavioristic study of the activity of the rat. *Comparative Psychology Monographs*, *1*, *2*, 56.

Riediger, C., Schuster, T., Barlinn, K., Maier, S., Weitz, J., & Siepmann, T. (2017). Adverse effects of antidepressants for chronic pain: A systematic review and meta-analysis. *Frontiers in Neurology*, *8*, 307. https://doi.org/10.3389/fneur.2017.00307

Sah, P., Faber, E. S. L., Lopez de Armentia, M., & Power, J. (2003). The amygdaloid complex: Anatomy and physiology. *Physiological Reviews*, *83*(3), 803–834. https://doi.org/10.1152/physrev.00002.2003

Salib, M., Joshi, A., Katona, L., Howarth, M., Micklem, B. R., Somogyi, P., & Viney, T. J. (2019). GABAergic medial septal neurons with low-rhythmic firing innervating the dentate gyrus and hippocampal area CA3. *The Journal of Neuroscience*, *39*(23), 4527–4549. https://doi.org/10.1523/JNEUROSCI.3024-18.2019

Saper, C. B. (2008). A guide to the perplexed on the specificity of antibodies. *Journal of Histochemistry & Cytochemistry*, *57*(1), 1–5. https://doi.org/10.1369/jhc.2008.952770

Schofield, B. R. (2008). Retrograde axonal tracing with fluorescent markers. *Current Protocols in Neuroscience*, *43*(1), 1.17.1–1.17.24. https://doi.org/10.1002/0471142301.ns0117s43

Schulz, D., & Canbeyli, R. (1999). Freezing behavior in BNST-lesioned Wistar rats. *Annals of the New York Academy of Sciences*, *877*(1), 728–731. https://doi.org/10.1111/j.1749-6632.1999.tb09311.x

Schulz, D., & Canbeyli, R. S. (2000). Lesion of the bed nucleus of the stria terminalis enhances learned despair. *Brain Research Bulletin*, *52*(2), 83–87. https://doi.org/10.1016/S0361-9230(00)00235-5

Shammah-Lagnado, S. J., Alheid, G. F., & Heimer, L. (2001). Striatal and central extended amygdala parts of the interstitial nucleus of the posterior limb of the anterior commissure: Evidence from tract-tracing techniques in the rat. *The Journal of Comparative Neurology*, *439*(1), 104–126. https://doi.org/10.1002/cne.1999

Silveira, M. C. L., Sandner, G., & Graeff, F. G. (1993). Induction of Fos immunoreactivity in the brain by exposure to the elevated plus-maze. *Behavioural Brain Research*, *56*(1), 115–118. https://doi.org/10.1016/0166-4328(93)90028-O

Simerly, R. B. (1990). Hormonal control of neuropeptide gene expression in sexually dimorphic olfactory pathways. *Trends in Neurosciences*, *13*(3), 104–110. https://doi.org/10.1016/0166-2236(90)90186-E

Smith, K. S., & Berridge, K. C. (2005). The ventral pallidum and hedonic reward: Neurochemical maps of sucrose "liking" and food intake. *The Journal of Neuroscience*, *25*(38), 8637–8649. https://doi.org/10.1523/JNEUROSCI.1902-05.2005

Smythe, J. W., Colom, L. V, & Bland, B. H. (1992). The extrinsic modulation of hippocampal theta depends on the coactivation of cholinergic and GABA-ergic medial septal inputs. *Neuroscience & Biobehavioral Reviews*, *16*(3), 289–308. https://doi.org/10.1016/S0149-7634(05)80203-9

Sofroniew, M. V. (1983). Direct reciprocal connections between the bed nucleus of the stria terminalis and dorsomedial medulla oblongata: Evidence from immunohistochemical detection of tracer proteins. *Journal of Comparative Neurology*, *213*(4), 399–405. https://doi.org/10.1002/cne.902130404

Somogyi, P., Katona, L., Klausberger, T., Lasztóczi, B., & Viney, T. J. (2014). Temporal redistribution of inhibition over neuronal subcellular domains underlies state-dependent rhythmic change of excitability in the hippocampus. *Philosophical Transactions of the Royal Society B: Biological Sciences*, *369*(1635), 20120518. https://doi.org/10.1098/rstb.2012.0518

Sun, N., & Cassell, M. D. (1993). Intrinsic GABAergic neurons in the rat central extended amygdala. *Journal of Comparative Neurology*, *330*(3), 381–404. https://doi.org/ 10.1002/cne.903300308

Sun, Y., Nguyen, A. Q., Nguyen, J. P., Le, L., Saur, D., Choi, J., … Xu, X. (2014). Cell-type-specific circuit connectivity of hippocampal CA1 revealed through cre-dependent rabies tracing. *Cell Reports*, *7*(1), 269–280. https://doi.org/10.1016/j.celrep.2014.02.030

Swaab, D. F. (2007). Sexual differentiation of the brain and behavior. *Best Practice & Research Clinical Endocrinology & Metabolism*, *21*(3), 431–444. https://doi.org/10.1016/j.beem.2007.04.003

Swanson, L. W., & Petrovich, G. D. (1998). What is the amygdala? *Trends in Neurosciences*, *21*(8), 323–331. https://doi.org/ 10.1016/s0166-2236(98)01265-x

Tóth, K., Freund, T. F., & Miles, R. (1997). Disinhibition of rat hippocampal pyramidal cells by GABAergic afferents from the septum. *The Journal of Physiology*, *500*(2), 463–474. https://doi.org/10.1113/jphysiol.1997.sp022033

Uchida, K., Otsuka, H., Morishita, M., Tsukahara, S., Sato, T., Sakimura, K., & Itoi, K. (2019). Female-biased sexual dimorphism of corticotropin-releasing factor neurons in the bed nucleus of the stria terminalis. *Biology of Sex Differences*, *10*(1), 6. https://doi.org/10.1186/s13293-019-0221-2

Unal, G., Crump, M. G., Viney, T. J., Éltes, T., Katona, L., Klausberger, T., & Somogyi, P. (2018). Spatio-temporal specialization of GABAergic septo-hippocampal neurons for rhythmic network activity. *Brain Structure and Function*, *223*(5), 2409–2432. https://doi.org/10.1007/s00429-018-1626-0

Unal, G., Joshi, A., Viney, T. J., Kis, V., & Somogyi, P. (2015). Synaptic targets of medial septal projections in the hippocampus and extrahippocampal cortices of the mouse. *The Journal of Neuroscience*, *35*(48), 15812–15826. https://doi.org/10.1523/JNEUROSCI.2639-15.2015

Vandecasteele, M., Varga, V., Berényi, A., Papp, E., Barthó, P., Venance, L., … Buzsáki, G. (2014). Optogenetic activation of septal cholinergic neurons suppresses sharp wave ripples and enhances theta oscillations in the hippocampus. *Proceedings of the National Academy of Sciences*, *111*(37), 13535–13540. https://doi.org/10.1073/pnas.1411233111

Viney, T. J., Lasztoczi, B., Katona, L., Crump, M. G., Tukker, J. J., Klausberger, T., & Somogyi, P. (2013). Network state-dependent inhibition of identified hippocampal CA3 axo-axonic cells in vivo. *Nature Neuroscience*, *16*(12), 1802–1811. https://doi.org/10.1038/nn.3550

Viney, T. J., Salib, M., Joshi, A., Unal, G., Berry, N., & Somogyi, P. (2018). Shared rhythmic subcortical GABAergic input to the entorhinal cortex and presubiculum. *ELife*, *7*, e34395. https://doi.org/10.7554/eLife.34395

Wainer, B. H., Levey, A. I., Rye, D. B., Mesulam, M.-M., & Mufson, E. J. (1985). Cholinergic and non-cholinergic septohippocampal pathways. *Neuroscience Letters*, *54*(1), 45–52. https://doi.org/10.1016/S0304-3940(85)80116-6

Walker, D. L., Miles, L. A., & Davis, M. (2009). Selective participation of the bed nucleus of the stria terminalis and CRF in sustained anxiety-like versus phasic fear-like responses. *Progress in Neuro-Psychopharmacology and Biological Psychiatry*, *33*(8), 1291–1308. https://doi.org/10.1016/j.pnpbp.2009.06.022

Walker, D. L., & Davis, M. (1997). Anxiogenic effects of high illumination levels assessed with the acoustic startle response in rats. *Biological Psychiatry*, *42*(6), 461–471. https://doi.org/10.1016/S0006-3223(96)00441-6

Wang, S.-M., Han, C., Bahk, W.-M., Lee, S.-J., Patkar, A. A., Masand, P. S., & Pae, C.-U. (2018). Addressing the side effects of contemporary antidepressant drugs: A comprehensive review. *Chonnam Medical Journal*, *54*(2), 101–112. https://doi.org/ 10.4068/cmj.2018.54.2.101

Weiskrantz, L. (1956). Behavioral changes associated with ablation of the amygdaloid complex in monkeys. *Journal of Comparative and Physiological Psychology*, *49*, 381–391. https://doi.org/10.1037/h0088009

Whishaw, I. Q., & Vanderwolf, C. H. (1973). Hippocampal EEG and behavior: Change in amplitude and frequency of RSA (theta rhythm) associated with spontaneous and learned movement patterns in rats and cats. *Behavioral Biology*, *8*(4), 461–484. https://doi.org/10.1016/S0091-6773(73)80041-0

Winson, J. (1978). Loss of hippocampal theta rhythm results in spatial memory deficit in the rat. *Science*, *201*(4351), 160–163. https://doi.org/10.1126/science.663646

Yizhar, O., Fenno, L., Zhang, F., Hegemann, P., & Diesseroth, K. (2011). Microbial opsins: A family of single-component tools for optical control of neural activity. *Cold Spring Harbor Protocols* , *2011*(3), top102. https://doi.org/10.1101/pdb.top102

Yoder, R. M., & Pang, K. C. H. (2005). Involvement of GABAergic and cholinergic medial septal neurons in hippocampal theta rhythm. *Hippocampus*, *15*(3), 381–392. https://doi.org/10.1002/hipo.20062

Záborszky, L., Cullinan, W. E., & Braun, A. (1991). Afferents to basal forebrain cholinergic projection neurons: An update. In T. C. Napier, P. W. Kalivas, & I. Hanin (Eds.), *The basal forebrain: Anatomy to function* (pp. 43–100). Springer, Boston, MA. https://doi.org/10.1007/978-1-4757-0145-6_2

Zaborsky, L., Pang, K., Somogyi, J., Nadasdy, Z., & Kallo, I. (1999). The basal forebrain corticopetal system revisited. *Annals of the New York Academy of Sciences*, *877*(1), 339–367. https://doi.org/10.1111/j.1749-6632.1999.tb09276.x

Zaborszky, L., van den Pol, A., & Gyengesi, E. (2012). Chapter 28 - The basal forebrain cholinergic projection system in mice. In C. Watson, G. Paxinos, & L. Puelles (Eds.), *The mouse nervous system* (pp. 684–718). Academic Press. https://doi.org/10.1016/B978-0-12-369497-3.10028-7

Zahm, D. S. (1989). The ventral striatopallidal parts of the basal ganglia in the rat—II. Compartmentation of ventral pallidal efferents. *Neuroscience*, *30*(1), 33–50. https://doi.org/10.1016/0306-4522(89)90351-5